

C H A P T E R   V

HARDNESS OF RHOMBOHEDRAL CRYSTALS :

SODIUM NITRATE AND CALCITE

# C H A P T E R V

## HARDNESS OF RHOMBOHEDRAL CRYSTALS : SODIUM NITRATE AND CALCITE

	PAGE
5.1 INTRODUCTION . . . . .	89
5.2 OBSERVATION . . . . .	94
5.3 RESULTS AND DISCUSSION . . . . .	94
5.3.1 VARIATION OF KNOOP HARDNESS NUMBER WITH APPLIED LOAD AT CONSTANT TEMPE- RATURE AND INDENTER ORIENTATION	94
5.3.2 VARIATION OF KNOOP HARDNESS NUMBER WITH QUENCHING TEMPERATURE FOR CONSTANT APPLIED LOAD IN HLR AND INDENTER ORIENTATION . . . . .	100
5.4 CONCLUSIONS . . . . .	105

TABLES

FIGURES

REFERENCES

## 5.1 INTRODUCTION:

From the discussion of previous chapter it is clear tht modified Kick's law is valid for cleavage faces of synthetic single crystals of  $\text{NaNO}_3$  for the entire range of applied loads whereas to a certain extent it is applicable to cleavage faces of natural  $\text{CaCO}_3$  crystals in the range of high loads only.

The present chapter reports detailed study of variation of hardness expressed by hardness number with quenching temperature and orientation of the knoop indenter with respect to crystal lattice. The knoop hardness number, H, is defined by the equation /1/.

$$H = 14230 P/d^2 \quad \dots \quad \dots \quad (5.1)$$

or

$$H = c P/d^2 \quad \dots \quad \dots \quad (5.2)$$

where applied load 'P' is in gm and the diagonal length 'd' of the indentation mark is in microns and  $c = 14230$  is a constant of the indenter geometry. This factor can be obtained in the following way from the general definition of knoop hardness number:

$$H \text{ (kg/mm}^2\text{)} = \frac{\text{Applied load P(kg)}}{\text{Projected area of the knoop indentation mark A (mm}^2\text{)}} \quad \dots \quad (5.2a)$$

The projected area A is given by

$$\begin{aligned} A &= \frac{1}{2} d^2 \cot \frac{172.5}{2} \tan \frac{130}{2} \\ &= \frac{1}{2} d^2 (0.0655)(2.1455) \\ &= d^2 (0.07028) \end{aligned}$$

where 'd' is in mm and  $172.5^\circ$  and  $130^\circ$  are the angles made by opposite edges of the indenter (cf. chapter III, Fig.3.1).

Thus,

$$\begin{aligned} H &= \frac{P}{A} = \frac{P}{0.07028 d^2} \\ &= 14.230 \frac{P}{d^2} \text{ kg/mm}^2. \end{aligned}$$

In the above formula P is in kg and d is in mm. In actual work P is in gm and d is in micron ( $\mu\text{m}$ ). Hence following the usual conversion, one obtains

$$H = 14230 P/d^2 \quad \dots \quad \dots \quad (5.3)$$

where P is in gm and d is in micron.

The hardness number H is not an ordinary number, but a constant having dimensions of stress and has a deep but less understood physical meaning. The combination of (5.2) with Meyer's law/Kick's law ( $P = ad^n$ ) yields

$$H = c.a.d^{n-2} \quad \dots \quad \dots \quad (5.4)$$

or in terms of applied load and hardness number it is given by

$$H = c.a^{2/n}.P^{n-2/n} \quad \dots \quad \dots \quad (5.5)$$

The above equation can be tested by comparing the values of left hand and right hand sides obtained from measurements. Thus H can be determined from (5.3) whereas on the right hand side the value of 'a' can be substituted from the earlier studies of the above laws (cf. chapter IV). Since c and P or d are known, the right hand side value can be calculated. Comparison of values obtained for the two sides of (5.4)/(5.5) can indicate the degree of correlation of the experimental work with the theoretical work.

Instead of using Kick's law, it is also possible to use modified Kick's law by putting  $n = 2$  and substituting  $(P-W)$  instead of  $P$  in the above formulae. Thus

$$\begin{aligned} H &= c \cdot \frac{P-W}{d^2} \\ (P-W) &= bd^2 \\ \therefore H &= cb \quad \dots \quad \dots \end{aligned} \quad (5.6)$$

Since  $c$  and  $b$  are constants, the above equation indicates that hardness is a constant quantity, independent of applied load and dimension of indentation mark. It was shown earlier (cf. chapter IV) that the modified Kick's law is independent of indenter (ball or pyramidal) geometry. Thus the above equation shows that the multiplication of geometrical constant (numerical figure) with ' $b$ ', the standard hardness, gives the hardness number. The present work aims at analysing the hardness behaviour by examining the relations (5.4), (5.5) and (5.6) experimentally. It also aims at studying quench hardness, variation of hardness with orientation and with effective resolved shear stress. It is mentioned above that the dimensions of hardness number and stress are the same. This similarity appears to have been obtained from the consideration of a solid subjected to uniaxial compression (or extension). For uniaxially compressed solid, the Young's modulus of elasticity ( $E$ ) is given by

$$E = \frac{\sigma}{\epsilon} \quad \dots \quad \dots \quad (5.7)$$

where  $\sigma$  is the compressive stress defined as load per unit area.

$$\sigma = \frac{P}{A} \quad \dots \quad \dots \quad (5.8)$$

and the compressive strain  $\epsilon$  is defined as the decrease in length

per unit length. The area of cross-section,  $A$ , increases with compression. Hence for a constant volume of a geometrically well-defined solid, length is inversely proportional to the area of cross-section. If  $A_0$  represents initial area of cross-section with a normal length  $l_0$ , and  $A$ , the final area with normal length  $l$  after small compression, one obtains,

$$l \cdot A = l_0 \cdot A_0$$

or,

$$\frac{l}{l_0} = \frac{A_0}{A} \quad \dots \quad \dots \quad (5.9)$$

Therefore,

$$\epsilon = (l - l_0)/l = (A_0 - A)/A \quad \dots \quad (5.10)$$

Substitution of  $\sigma$  and  $\epsilon$  from (5.8) and (5.10) in (5.7) gives,

$$E = P/(A_0 - A) \quad \dots \quad \dots \quad (5.11)$$

Hence, for a simple uniaxial compressive stress, when the area is a geometrical function of deformation, determined here by constant volume, the resistance to permanent deformation can be expressed simply in terms of load and corresponding area. In indentation process, the volume change is very very small; volume of solid can therefore be considered as constant. Hence the indentation hardness can be measured by using the above formula (5.11).

Indenters are made in various geometrical shapes such as spheres, pyramids, etc. The area over which the force due to load on indenter acts, increases with the depth of penetration. The resistance to permanent deformation or hardness can be expressed in terms of force or load and area alone (and/or depth of penetration). These remarks are true for solids which are amorphous or highly homogeneous and isotropic.

The above analysis presents a highly simplified picture of the processes involved because there is a great difference between deforming a solid in a simple uniaxial compression and deforming a surface of a solid by pressing a small indenter into it. Around the indentation mark, the stress distribution is exceedingly complex and the stressed material is under the influence of multiaxial stresses. The sharp corners of a pyramidal indenter produces a sizable amount of plastic deformation which may reach 30% or more at the tip of the indenter. Further the surface of contact is inclined by varying amounts to the directions of applied force. In view of these complications a simple expression corresponding to that for the modulus of elasticity can not be derived for hardness. In the absence of any formula based on concrete theory, an arbitrary expression is used which includes both known variables - load and area - in the present case. Hence the hardness number, H, is defined as the ratio of the load to the area of impression,

$$H = P/A \quad \dots \quad \dots \quad \dots \quad (5.12)$$

For pyramidal indenters the load P varies as the square of the diagonal d. Thus for a given shape of pyramid,

$$P = ed^2 \quad \dots \quad \dots \quad \dots \quad (5.13)$$

where 'e' is a constant which depends on the material and shape of pyramid. The area of the impression, A, is also proportional to the square of the diagonal,

$$A = fd^2 \quad \dots \quad \dots \quad \dots \quad (5.14)$$

where 'f' depends upon the shape of the pyramid. Combination of equations 5.12, 5.13 and 5.14 gives,

$$H = ed^2/fd^2 = e/f = \text{constant} \dots \quad (5.15)$$

Hence for a given shape of pyramidal indenter, hardness is independent of load and size of indentation. This statement represents Kick's

law. In view of defining equation (5.2a) for hardness, hardness number can also be considered as hardening modulus.

Due to complicated behaviour of indented anisotropic single crystals of various materials and arbitrary expression for hardness, it is clear that the theoretical treatment of the problem is extremely difficult. Hence it is desirable to approach this problem via experimental observations, interpretations and with a probable development of empirical relation(s). Further the analysis can be used for developing model theory/theories of hardness. The present work is taken up from this phenomenological point of view and is an extension of the work carried out by Saraf /2/, Mehta /3/, Shah /4/, Acharya /5/, Bhagia /6/, Shah /7/ and Patel /8/ in this laboratory.

## 5.2 OBSERVATIONS:

The observations which were recorded for studying the Kick's law/Meyer's law ( $P = ad^n$ ) are used in the present investigation. The Knoop hardness numbers are calculated using equation (5.1) for various orientations and for the thermally treated and untreated samples. The observations are graphically studied by plotting the graph of hardness number  $H$  versus load  $P$  (cf. Fig.5.1, 5.2) In what follows the hardness and Knoop hardness number will be used to indicate the same meaning.

## 5.3 RESULTS AND DISCUSSION:

### 5.3.1 Variation of Knoop Hardness Number with applied load at constant temperature and indenter orientation:

It is clear from the graphical analysis of the variation of hardness number  $H$  with load  $P$  (Figs.5.1, 5.2) that contrary to theoretical expectations, the hardness varies with load. For calcite the hardness at first increases with load for all orientations and

for all quenching temperatures, reaches a maximum value at a certain load, then gradually decreases with increasing load and attains almost a constant value for all higher applied loads. For  $\text{NaNO}_3$ , the nature of the plot of  $H$  Vs.  $P$  is slightly different. Initially for lower loads, the hardness is maximum, decreases gradually with increasing load and attains a constant value for all higher loads. The complex behaviour of microhardness with load can be explained qualitatively on the basis of depth of penetration of the indenter. At small loads the indenter penetrates only surface layers, hence the effect is shown more sharply at these loads. However, as the depth of penetration (impression) increases, the effect of surface layers becomes less dominant and after a certain depth of penetration, the effect of inner layers becomes more and more prominent than those of surface layers and ultimately there is practically no change in the value of hardness with load. This is apparent from the graphs of Knoop hardness number Vs. load.

It is clear from the plots of  $H$  Vs.  $P$  that the theoretical conclusion that hardness is independent of load appears to be true only at higher loads. The maximum value of hardness for calcite corresponds with a load which is nearer the value of the load at which kink in the graph of  $\log d$  Vs.  $\log P$  is observed (cf. chapter IV). Whereas for  $\text{NaNO}_3$ , this type of behaviour is not at all observed. For calcite crystals, the graph of  $H$  Vs.  $P$  can be conveniently divided into three parts, AB, BC and CD, where the first part represents linear relation between hardness and load, the second part, the non-linear relation and the third part the linear one. It should be noted that there is a fundamental difference between linear portions AB and CD of the graph ABCD. This possibly reflects varied reactions of the cleavage surface to loads belonging to different regions. Besides it supports, to a certain extent, the earlier view about the splitting of graph of  $\log d$  Vs.  $\log P$  into two recognizable straight lines corresponding to low load and high load regions (namely, LLR and HLR)(cf, chapter IV).

Contrary to the above picture, only two regions are observed for  $\text{NaNO}_3$  crystals, which are designated as non-linear BC portion and linear CD portion of the graph of H Vs. P. The maximum value of hardness in both the cases is represented by B.

The present approach for the study of hardness behaviour with a change in different parameters is an integrated one. Hence the graphical analysis of  $\log d$  Vs.  $\log P$  plots (cf. chapter IV) should now be extended in the present work by studying the relations (5.4), (5.5) and (5.6), namely,

$$(5.4) \quad \dots H = C a d^{n-2}$$

$$(5.5) \quad \dots H = C a^{(2/n)} P^{(n-2)/n}$$

$$(5.6) \quad \dots H = C b$$

for  $\text{CaCO}_3$  and  $\text{NaNO}_3$ .

For calcite cleavages there exists two distinct ranges of applied load, viz., LLR and HLR corresponding to plot of  $\log d$  Vs.  $\log P$  consisting of two straight lines with different slopes ( $n_1$  &  $n_2$ ) and intercepts ( $\log a_1$  &  $\log a_2$ ), whereas the plot of H Vs. P (Fig.5.1, 5.2) shows three ranges of applied loads, namely, low load region LLR, intermediate load region ILR and high load region HLR designated by AB, BC and CD respectively and that CD corresponds to that range of applied loads where hardness number calculated by using equation (5.1) is constant and independent of applied load. Assuming that modified Kick's law is valid for the hardness formula, the plot of H (calculated by using  $H = 14230 \frac{P-W}{d^2}$  and shown in table 5.5) Versus (P - W) also shows CD as the HLR where hardness is constant and independent of load. HLR is common for both plots (Fig.5.3). Further it is clear from the plots that for applied loads greater than 20 gm for  $\text{NaNO}_3$  and 40 gm for  $\text{CaCO}_3$  hardness is constant and independent of load. It is in this range of applied

loads for which the hardness behaviour of these crystals is analysed and reported in the present work.

Values of hardness for  $\text{NaNO}_3$  obtained from the graph (Fig.5.1) and calculated by using relations (5.5) and (5.6) at different quenching temperatures and indenter orientations are given in tables 5.3 A, 5.3 B and 5.3 C, respectively. The comparison of hardness values for constant temperature and indenter orientation show very clearly that within experimental errors there is no wide difference between them. By considering the graphical value as standard, calculations are made for constant temperature and indenter orientation, about the percentage deviations of hardness values (cf. table 5.3 D (i) & (ii)). It is obvious that for all practical purposes the deviations are not significant (table 5.3 D). It can therefore be concluded that cleavage faces of  $\text{NaNO}_3$  obey the Meyer's law/Kick's law and modified Kick's law for constant temperature and orientation.

It was shown in the earlier chapter that for calcite cleavages the straight line plot of  $\log d$  Vs.  $\log P$  consists of two straight lines with different slopes and intercepts corresponding to LLR & HLR. The slope and intercept in this region (HLR) are  $n_2$  and  $a_2$ , respectively. In the case of modified Kick's law  $b_2$  corresponds to  $a_2$  and  $n_2 = 2$  and the law is approximately applicable. The plot of  $H$  Vs.  $P$  indicates three regions LLR, ILR & HLR and that HLR corresponds to applied loads greater than 40 gm. Further, it is this region where hardness is almost constant and independent of load. It is therefore desirable to consider the following relations:

$$H = Ca_2 d^{n_2-2} \dots \dots \dots (5.7)$$

$$H = Ca_2^{2/n_2} \cdot P^{(n_2-2)/n_2} \dots \dots \dots (5.8)$$

$$H = Cb_2 \dots \dots \dots 95.9)$$

instead of 5.4, 5.5 & 5.6 and try to find the correlation amongst these relations. The observed graphical values of hardness (table

5.4 A) can now be compared with the values of hardness at constant temperature and orientation, calculated from the formulae (5.8) & (5.9) and presented in a tabular form (tables 5.4 B & 5.4 C). Table 5.4 D indicates percentage deviations of hardness values (tables 5.4 B & 5.4 C) from the observed values (table 5.4 A). It is clear from table 5.4 D that percentage deviation is very large indicating very little correlation between hardness values (tables 5.4 A, 5.4 B, 5.4 C). It can be concluded that hardness behaviour of calcite cleavages at constant temperature and orientation indicates little correlation amongst Meyer's law/Kick's law, modified Kick's law and formula for hardness number.

It is now desirable to apply the above analysis to hardness studies of  $\text{CaCO}_3$  and  $\text{NaNO}_3$  made by earlier workers in this laboratory /6,7,9/. They had utilized Vickers and Knoop indenters on cleavage faces of these crystals. Hardness was determined along direction [100], i.e., longer diagonal of Knoop indenter or a diagonal of Vickers indenter was parallel to [100]. Comparison of their results with those obtained in the present investigation suggests that indenter geometry does not change the behavioural pattern but values of Knoop hardness number and Vickers hardness number for a given applied load and constant temperature are significantly different from each other for calcite cleavages /6/. Hence it can be concluded that irrespective of the indenter geometry Meyer's law/Kick's law, modified Kick's law and hardness formula can not be experimentally correlated with one another for natural calcite crystals.

In the present investigation the straight line plot of  $\log d$  Vs.  $\log P$  consists of a single straight line for  $\text{NaNO}_3$  cleavage faces obtained from a synthetic  $\text{NaNO}_3$  single crystals grown by using fine (spectroscopically pure) quality of  $\text{NaNO}_3$ . It was reported /7,9/ that the straight line plot consists of two distinct straight lines with different slopes ( $n_1, n_2$ ) and intercepts ( $\log a_1, \log a_2$ ). This was found to be due to the use of commercial (impure) quality of  $\text{NaNO}_3$  for growing crystals. Knoop and Vickers indenters were used to study hardness of these crystals. The first part of the graph

corresponds to LLR and hence only second part of the plot has to be considered. When the graph of  $H$  Vs.  $P$  is considered along with this straight line plot, it was observed that at a constant temperature hardness for applied loads greater than 20 gm is constant, independent of applied load and independent of indenter geometry. Thus HLR for loads greater than 20 gm is to be considered in the present analysis. Expressions of Kick's law and hardness number are combined as usual. The mean graphical values of hardness designated for Knoop and Vickers indenters by  $H_k$  &  $H_v$  and also  $H_k$  &  $H_v$  values calculated from the formulae (5.8) & (5.9) are given in table (5.6) A & B. A careful glance at the table indicates that hardness values obtained from the plots are slightly different from those calculated by using (5.8). However, there are significantly wide variations between values obtained from plots and calculated by using (5.9). This relation is a combination of modified Kick's law and hardness expression for Knoop or Vicker's indenter. In this the values of 'b' & 'w' for Knoop and Vicker's indenter are calculated by exactly following the procedure narrated in chapter IV and are given in table (5.6) A & B. It is thus clear that impurity in the material plays a very important role in the hardness work and appears to dominate in exhibiting the splitting of the straight line plot of  $\log d$  Vs.  $\log P$  into two straight lines. It is therefore concluded that at a constant temperature and orientation hardness number (Knoop or Vickers) is affected very much by the impurity content of the base material and that for an impured material from which the single crystals are grown, the modified Kick's law does not hold. Besides, there are several factors such as anisotropy, imperfections and their interactions, introduction of additional imperfections on indentation and their interactions among themselves and with the grown-in imperfections, range of hardness numbers, etc., which should be acting in a way unpredictable from the present study.

**5.3.2 Variation of Knoop hardness number with quenching temperature for constant applied load in HLR and indenter orientation:**

It is clear from the observations of hardness of quenched and unquenched samples (tables 5.3 A & 5.4 A) that hardness depends upon the quenching temperature  $T_q$  and that in HLR it is independent of load. Hence average values of hardness  $\bar{H}$  in HLR are computed and are recorded in tables 5.3 A & 5.4 A. For  $\text{NaNO}_3$  and  $\text{CaCO}_3$  the tables of  $\log \bar{H}T_q$  &  $\log T_q$  are prepared (Tables 5.7 & 5.8) from the observations (vide tables 5.3 A & 5.4 A). The plots of  $\log \bar{H}T_q$  versus  $\log T_q$  are straight lines (Figs.5.4 & 5.5) for different quenching temperatures and different orientations of indenter. It should be noted that the plots are shown for all orientations of indenter with respect to [100] direction for  $\text{NaNO}_3$  and  $\text{CaCO}_3$ . The slopes of these lines for  $\text{NaNO}_3$  and  $\text{CaCO}_3$  cleavages are given in tables 5.7 and 5.8. The straight line graph follows the equation,

$$\text{Log } \bar{H}T_q = m \log T_q + \log C \quad \dots \quad (5.16)$$

where 'm' is the slope and  $\log C$  is an intercept. Therefore,

$$\begin{aligned} \bar{H}T_q^{1-m} &= C \\ \text{or } \bar{H}T_q^K &= C \quad \dots \quad \dots \quad (5.17) \end{aligned}$$

where,  $K = 1 - m$ . The values of  $K$  are given for  $\text{NaNO}_3$  and  $\text{CaCO}_3$  for different directions in tables 5.7 & 5.8.

The comparison of the changes and also percentage changes in the variation of hardness of  $\text{NaNO}_3$  and  $\text{CaCO}_3$  with quenching temperatures and for different orientations of indenter with reference to [100] direction show that these variations are more for calcite than for  $\text{NaNO}_3$ .

For  $\text{NaNO}_3$  and  $\text{CaCO}_3$  cleavages

$$\bar{H}T_q^K = C$$

for all indenter orientations and applied loads in the HLR where hardness is constant and independent of load. 'K' is a number which is much less than unity and +ve for  $\text{NaNO}_3$  and -ve for  $\text{CaCO}_3$ . This shows that quench hardness increases with decreasing quenching temperature for  $\text{NaNO}_3$  and increases with increasing temperature for calcite. In both these cases the change from room temperature value is quite small. This change is made detectable due to fine combination of determinable/measurable variables involved in the experiments on quench hardness studies. Further K values for  $\text{NaNO}_3$  changes with orientation and is the lowest for  $39^\circ$  orientation which represents the projection of optic axis  $[\bar{1}\bar{1}1]$  on a cleavage plane of  $\text{NaNO}_3$ . Such uniform variation is not observed for  $\text{CaCO}_3$ . The value of exponent K or slope of the straight line plots of  $\log \bar{H}T_q$  Vs.  $\log T_q$  (Fig.5.4, 5.5) is so small that all of them appear to be parallel lines. However, close examination of these plots show them to be slightly unparallel. Small value of K indicates that variation of quenched hardness with quenching temperature is quite small. This is due to the fact that after quenching the surface layers get more affected. Hence these layers are removed by cleaving the crystal ( $\text{NaNO}_3/\text{CaCO}_3$ ). It is therefore clear that whatever effect the quenching process has produced in the crystal, it will be body effect and not surface effect. Quench hardness thus determined represents 'body' hardness or of the highly deep interior layers. Obviously quench hardness will not differ very much from room temperature hardness. This is found to be the case for all crystals studied in this laboratory. The constant C for  $\text{NaNO}_3$  and  $\text{CaCO}_3$  cleavages changes with indenter orientation. The variations are such that value of C becomes a minimum in the direction of  $[\bar{1}\bar{1}0]$  of the indenter orientation with reference to  $[100]$ . Thus the exponent and constant have very small values when the angle between the indenter major diagonal and  $[100]$  direction is  $39^\circ$ . This represents the direction  $[\bar{1}\bar{1}0]$ , along with homogeneous isotropic character of  $\text{NaNO}_3/\text{CaCO}_3$  is observed. Thus the quench hardness study on cleavage faces of  $\text{NaNO}_3/\text{CaCO}_3$  has clearly shown that these crystals

obey the relation

$$H_A T_q^{K_A} = \text{constant} = C_A$$

and that  $K_A$  and  $C_A$  change with crystalline anisotropy.  $K_A$  and  $C_A$  have small values when the major diagonal of indenter makes an angle of  $39^\circ$ , i.e., when it is in direction  $[\bar{1}\bar{1}0]$ .

For a range of loads in HLR hardness is inversely proportional to the square of the length of major diagonal. Hence instead of plotting a graph of  $\log H_A T_q$  Vs.  $\log T_q$  it is possible to plot a graph of  $\log T_q d$  Vs.  $\log T_q$ . This should result in a straight line plot and the equation for this plot should yield, after simplification, the values of  $C_A$  and  $K_A$ . The plot of the above mentioned graphs for a range, say  $r$ , of applied loads in HLR, are straight lines parallel to each other for a constant orientation of the indenter. For different orientations, the plots consist of a series of parallel straight lines with different intercepts. A typical set of parallel plots for constant orientation of the indenter ( $A = 0^\circ$ ) is shown in the Fig.5.6. The straight line equation for such parallel plots will have the form,

$$\log T_q d = m_A \log T_q + \log C_A$$

where  $m_A$  is the slope of these parallel straight lines making different intercepts  $\log C_{A1}$ ,  $\log C_{A2}$ , .....,  $\log C_{Ar}$  for 'r' parallel lines.

Rewriting corresponding to orientations  $A_1$ ,  $A_2$ , .....,  $A_r$ ; the above equation for one of the parallel lines and one value of orientation, give-

$$\log T_q d_{Ar} = m_A \log T_q + \log C_{Ar}$$

$$d_{Ar} T_q = C_{Ar} T_q^{m_A}$$

$$d_{Ar} T_q^{1-m_A} = C_{Ar} \dots \dots \dots (5.18)$$

The above relation should be connected with (5.17), namely,

$$H_A T_q^{K_A} = H_A T_q^{1-m} = C_A \dots \dots \dots (5.17)$$

where  $H_A$  is hardness for different orientations A. Now combination of the above with (5.1) results into-

$$\frac{14230 P}{d^2} T_q^{1-m} = C_A$$

$$d^2 T_q^{m-1} = \frac{14230 P}{C_A}$$

Taking the square-root and retaining +ve sign before the square root, one gets,

$$d T_q^{(m-1)/2} = \sqrt{\frac{14230 P}{C_A}} \dots \dots \dots (5.19)$$

The relations (5.18) and (5.19) can be considered identical of

$$1 - m_A = \frac{m-1}{2} = \frac{K_A}{2}$$

$$\text{and } C_{Ar} = \sqrt{\frac{14230 P}{C_A}}$$

Since  $r$  represents range of applied loads corresponding to longer diagonals  $d_r$ , the values of  $P$  on R.H.S. of the above equation are different. Hence to indicate this for a range  $r$  of applied loads the above equations can be rewritten in a generalized form-

$$1 - m_{Ar} = \frac{m_A^{-1}}{2} = \frac{K_A}{2}$$

$$C_{Ar} = \sqrt{\frac{14230 P_r}{C_A}} = d_{Ar} T_q^{K/2}$$

Thus for different values of applied load  $P_r$ , i.e., for different values of  $r$ , there will be series of values of  $C_{Ar}$  and  $d_{Ar}$ .

Further,

$$\frac{C_{Ar}^2}{P_r} = \frac{14230}{C_A}$$

or

$$\frac{C_{Ar}}{P_r} = \sqrt{\frac{14230}{C_A}}$$

Calculation of values on the L.H.S. and R.H.S. are made by using the relations for  $d$  &  $H$ , i.e., (5.18) & (5.17) and are shown in the Fig.(5.6). The table (5.9) indicates that within experimental limits, these values are fairly in agreement with each other.

It is thus clear that for various applied loads  $P_r$  in the high load region, the relation between the longer diagonal of the Knoop indentation mark,  $d_{Ar}$ , quenching temperature  $T_q$  and indenter orientation  $A$  (typical set of observations is given in Table 5.10), is given by,

$$d_{Ar} T_q^{K_A/2} = \sqrt{\frac{14230 P_r}{C_A}}$$

#### 5.4 CONCLUSIONS:

- (1) Hardness varies with load. For calcite it increases initially with load for all orientations and for all quenching temperatures, reaches a maximum value at a certain load, then gradually decreases with increasing loads and attains almost a constant value for all higher applied loads. For  $\text{NaNO}_3$ , the hardness is maximum initially for lower loads, decreases gradually with increasing load and attains a constant value for all higher loads. This behaviour reflects varied reactions of cleavage surfaces of  $\text{CaCO}_3$  and  $\text{NaNO}_3$  to applied loads.
- (2) (a) Cleavage faces of  $\text{NaNO}_3$  obey Meyer's law/Kick's law and modified Kick's law at constant temperature and orientation of indenter with respect to direction [100].  
 (b) Irrespective of the indenter geometry, Meyer's law/Kick's law, modified Kick's law and hardness formula can not be experimentally correlated with one another for natural calcite crystals.
- (3) Hardness is affected very much by the impurity content of the base material and that for a single crystal grown from such a material, the modified Kick's law does not hold.
- (4) For  $\text{NaNO}_3$  and  $\text{CaCO}_3$  cleavages,  $H_A^{TK} = C_A$  for all indenter orientations and applied loads in the high load region where hardness is constant and independent of load. Quenched hardness ( $H_A$ ) represents body hardness or the effects of layers highly deep inside a crystal. It does not differ very much from the room-temperature hardness of untreated crystals. The constant  $C_A$  for  $\text{NaNO}_3$  and  $\text{CaCO}_3$  cleavages changes with indenter orientation with respect to direction [100] and has a minimum value in the direction  $[\bar{1}\bar{1}0]$  of the indenter orientation with reference to [100].  $K$  and  $C_A$  change with crystalline anisotropy.

- (5) For  $\text{NaNO}_3$  and  $\text{CaCO}_3$ , the relation between the longer diagonal of Knoop indentation mark  $d_{Ar}$  corresponding to different applied loads  $P_r$  in the high load region and quenching temperature  $T_q$  and orientation  $A$  of the indenter is given by-

$$d_{Ar} T_q^{K_A/2} = \sqrt{\frac{14230 P_r}{C_A}}$$

TABLE 5.1 (i)

(for  $\text{NaNO}_3$ )Room Temperature :  $T_1 = 298^\circ\text{K}$ 

Load P in gm.	Hardness H in $\text{kg-mm}^{-2}$						
	$0^\circ$	$13^\circ$	$26^\circ$	$39^\circ$	$52^\circ$	$65^\circ$	$78^\circ$
1.25	34.07	29.68	26.08	26.08	15.14	29.68	31.76
2.5	31.78	28.89	28.89	26.38	21.37	26.38	28.89
3.75	28.53	26.49	27.48	24.66	22.26	23.82	26.49
5.0	26.08	26.08	23.10	23.10	22.44	23.10	26.92
6.25	28.05	27.25	23.25	21.95	21.95	23.12	26.49
7.5	25.68	25.68	22.18	21.67	22.18	22.18	24.42
8.75	26.50	24.70	22.09	22.09	21.62	21.62	24.70
10.0	26.38	23.67	22.25	20.94	20.14	22.25	25.24
11.25	26.64	24.04	23.11	20.61	20.23	20.99	24.53
12.5	26.71	24.23	21.68	20.92	19.18	21.29	24.23
13.75	26.65	23.01	21.83	20.75	19.42	20.75	24.73
15.0	24.23	23.82	22.26	20.84	19.87	20.84	24.66
16.25	24.94	22.95	19.05	20.23	19.63	20.86	26.72
17.5	25.12	22.82	19.63	20.22	19.63	20.52	26.41
18.75	25.24	22.31	20.44	20.44	18.79	19.32	24.07
20.0	24.16	22.77	20.61	19.78	18.99	19.51	24.16
25.0	24.39	22.23	19.38	18.92	18.48	20.10	23.74
30.0	23.54	22.18	19.14	18.93	18.53	20.23	22.98
40.0	23.18	20.95	18.15	19.02	17.82	19.20	22.71
50.0	23.12	21.10	18.55	18.09	17.65	19.18	22.90
60.0	22.44	20.68	17.45	17.08	17.72	18.82	22.07
70.0	22.64	21.30	17.42	16.62	16.62	18.54	22.30
80.0	22.122	20.47	17.23	16.48	17.12	18.74	21.49
100.0	21.54	20.23	17.24	16.30	17.05	18.59	21.26
120.0	21.79	19.78	16.86	16.02	16.43	18.23	21.54
140.0	21.28	19.67	16.96	16.40	16.64	17.12	21.05
160.0	21.37	19.85	16.37	15.95	16.51	18.49	21.15

TABLE 5.1 (ii)

(for  $\text{NaNO}_3$ )Quenching Temperature :  $T_{q_1} = 343^\circ\text{K}$ 

Load P in gm.	Hardness H in $\text{kg-mm}^{-2}$						
	$0^\circ$	$13^\circ$	$26^\circ$	$39^\circ$	$52^\circ$	$65^\circ$	$78^\circ$
1.25	34.07	34.07	27.79	27.79	29.68	29.68	20.61
2.5	31.78	30.29	26.38	26.38	24.18	26.38	20.54
3.75	28.53	28.53	23.82	25.55	24.66	24.66	23.82
5.0	28.72	26.09	23.80	23.80	24.53	25.29	23.80
6.25	28.05	25.06	22.53	23.12	23.12	25.06	24.39
7.5	27.75	24.43	21.67	22.18	21.67	25.68	23.26
8.75	26.50	24.15	21.62	21.62	21.62	25.88	23.08
10.0	26.98	23.68	21.37	21.80	21.80	25.24	23.67
11.25	26.64	23.11	20.61	21.80	20.99	24.53	24.04
12.5	26.19	23.33	20.56	22.07	20.92	23.77	25.67
13.75	25.67	23.01	20.75	22.21	21.10	23.84	25.19
15.0	25.56	22.64	20.19	21.53	21.53	23.02	24.66
16.25	25.81	22.59	19.93	21.19	21.53	22.59	23.33
17.5	25.54	22.83	19.93	20.52	21.46	22.83	23.93
18.75	24.46	23.34	20.16	21.04	21.04	22.65	24.07
20.0	24.16	22.12	19.51	20.61	20.32	21.80	24.16
25.0	24.39	21.95	18.93	20.35	19.15	22.82	24.39
30.0	23.55	20.93	18.94	19.78	19.14	22.18	22.98
40.0	23.43	20.95	18.67	19.38	19.20	22.48	22.48
50.0	23.12	20.38	18.39	19.34	18.71	21.68	22.48
60.0	23.02	20.52	18.54	19.11	18.82	21.36	22.63
70.0	23.37	19.78	18.16	19.21	18.28	21.46	22.12
80.0	21.96	20.19	18.26	18.87	17.45	21.34	21.65
100.0	22.38	19.62	18.06	18.70	17.34	19.27	21.00
120.0	22.05	19.79	17.85	18.53	17.21	19.35	21.05
140.0	21.85	19.67	17.54	18.69	17.45	19.87	19.97
160.0	21.92	19.2	17.66	18.93	15.27	19.29	20.54

TABLE 5.1 (iii)

(for  $\text{NaNO}_3$ )Quenching Temperature :  $T_{q_2} = 393^\circ\text{K}$ 

Load P in gm.	Hardness H in $\text{kg-mm}^{-2}$						
	$0^\circ$	$13^\circ$	$26^\circ$	$39^\circ$	$52^\circ$	$65^\circ$	$78^\circ$
1.25	18.49	26.087	21.81	21.80	21.80	21.80	21.80
2.5	21.37	24.18	21.37	23.18	19.75	22.25	21.37
3.75	23.02	23.82	22.26	20.19	20.84	23.82	22.26
5.0	25.29	23.11	20.05	20.61	19.51	23.10	23.10
6.25	24.39	22.52	20.87	19.38	20.87	21.95	22.52
7.5	25.04	22.18	19.78	18.53	20.23	22.18	23.26
8.75	23.08	22.09	19.87	19.47	19.07	21.62	23.08
10.0	21.80	21.80	19.75	19.38	19.38	23.18	22.25
11.25	24.04	22.22	19.16	19.16	19.86	23.56	22.22
12.5	23.33	21.29	20.19	18.86	20.19	22.07	22.90
13.75	22.21	21.83	19.74	18.50	19.42	21.83	22.21
15.0	21.18	21.53	19.56	18.96	18.96	20.84	22.26
16.25	21.53	21.53	18.77	19.34	19.05	21.87	22.22
17.5	23.18	21.14	18.81	19.08	19.08	21.46	22.12
18.75	21.66	20.73	18.79	18.29	18.79	21.34	21.34
20.0	21.49	20.61	18.99	18.25	18.25	21.49	21.19
25.0	20.87	20.87	18.48	17.75	18.92	20.35	20.87
30.0	20.23	20.23	18.13	17.75	18.53	20.93	20.69
40.0	20.74	20.34	17.18	17.66	18.32	19.95	20.34
50.0	20.73	20.19	17.09	17.09	17.80	20.19	20.02
60.0	20.03	19.56	17.07	15.45	17.20	20.03	20.51
70.0	20.52	19.21	16.95	17.19	16.62	19.78	20.52
80.0	19.38	19.64	16.90	15.69	15.98	18.99	20.32
100.0	19.86	19.27	16.39	16.21	16.58	19.27	20.23
120.0	19.14	19.46	16.43	15.40	16.27	19.24	19.78
140.0	19.67	19.17	16.33	16.18	15.81	19.37	19.37
160.0	19.57	18.49	16.08	15.34	15.67	18.49	19.85

TABLE 5.1 (iv)

(for  $\text{NaNO}_3$ )Quenching Temperature :  $T_{q_3} = 443^\circ\text{K}$ 

Load P in gm.	Hardness H in $\text{kg-mm}^{-2}$						
	0°	13°	26°	39°	52°	65°	78°
1.25	21.80	20.61	23.10	19.51	24.54	29.68	26.08
2.5	24.18	25.24	23.18	21.37	24.18	25.24	23.19
3.75	24.66	23.82	22.26	20.84	22.26	23.82	22.26
5.0	23.11	23.80	21.20	19.51	21.19	24.53	23.11
6.25	23.74	22.52	19.38	19.86	19.86	23.12	22.52
7.5	24.43	21.17	19.78	18.13	20.23	20.69	22.18
8.75	22.58	21.16	20.29	18.69	19.87	18.13	22.09
10.0	23.19	22.25	19.38	18.32	19.76	21.37	21.80
11.25	23.10	22.23	19.51	18.17	19.51	21.39	21.80
12.5	22.90	22.07	19.18	18.24	20.19	21.29	22.48
13.75	22.61	21.84	19.11	18.21	20.07	21.46	22.21
15.0	22.26	21.53	18.96	18.67	19.56	21.53	21.89
16.25	22.22	21.87	18.50	17.97	18.77	20.86	22.22
17.5	22.47	21.14	18.29	18.03	18.54	21.46	22.12
18.75	22.31	22.31	17.57	17.81	18.29	21.35	21.98
20.0	22.12	20.61	17.56	17.79	17.79	20.32	21.50
25.0	21.40	20.35	17.05	17.44	17.24	20.10	21.13
30.0	21.42	20.01	17.39	17.21	17.75	20.46	21.42
40.0	20.95	19.95	16.88	16.58	17.18	19.75	20.34
50.0	21.10	19.34	17.09	16.69	16.43	19.34	20.19
60.0	21.01	19.26	16.48	15.67	16.95	18.96	20.19
70.0	20.67	19.35	16.62	15.87	15.77	18.41	19.78
80.0	21.04	19.38	16.38	15.89	15.23	18.99	19.64
100.0	20.87	19.62	16.21	16.04	16.95	18.81	20.10
120.0	20.34	19.14	15.55	15.25	16.02	19.14	19.24
140.0	20.50	19.08	15.59	15.81	16.18	18.69	19.17
160.0	20.24	19.38	15.61	15.15	16.23	18.66	19.20

TABLE 5.1 (v)

(for  $\text{NaNO}_3$ )Quenching Temperature :  $T_{q_4} = 493^\circ\text{K}$ 

Load P in gm.	Hardness H in $\text{kg-mm}^{-2}$						
	$0^\circ$	$13^\circ$	$26^\circ$	$39^\circ$	$52^\circ$	$65^\circ$	$78^\circ$
1.25	27.79	23.10	19.51	19.51	20.61	27.81	29.68
2.5	27.59	25.24	19.75	20.54	21.37	22.25	23.19
3.75	25.55	22.26	20.84	19.56	20.85	20.85	23.83
5.0	24.53	21.80	20.61	18.99	21.19	21.20	21.80
6.25	24.39	22.52	19.86	18.48	19.86	20.36	23.74
7.5	23.83	22.71	19.78	18.93	19.78	19.78	22.71
8.75	24.14	22.09	19.07	18.69	20.71	19.08	22.09
10.0	23.67	21.37	19.38	19.02	19.76	19.38	21.37
11.25	24.04	22.66	19.86	20.92	18.83	19.51	21.80
12.5	22.90	22.07	18.86	19.18	19.85	19.18	22.07
13.75	23.01	22.21	18.80	18.80	19.74	19.74	21.10
15.0	23.82	22.26	18.68	18.96	19.56	19.56	21.19
16.25	24.11	22.58	18.23	19.05	19.05	18.77	21.53
17.5	23.55	21.79	18.54	18.54	19.08	18.81	21.46
18.75	23.71	21.98	18.79	17.80	19.32	19.05	21.35
20.0	23.75	21.49	18.99	17.79	18.99	18.99	21.50
25.0	22.82	21.13	18.27	16.30	18.48	18.27	20.61
30.0	21.42	20.93	18.53	17.21	18.73	18.73	20.46
40.0	21.37	20.74	17.82	16.73	17.66	17.66	20.34
50.0	22.07	21.10	16.69	17.80	17.65	18.55	20.02
60.0	21.01	20.68	16.35	15.67	17.58	16.95	19.71
70.0	21.62	20.52	16.18	16.40	17.54	18.41	19.78
80.0	21.80	20.32	16.90	15.89	17.45	18.37	19.78
100.0	20.87	20.48	16.48	16.04	17.64	17.44	19.62
120.0	20.34	20.00	15.86	15.63	17.30	16.86	19.14
140.0	20.50	19.57	15.95	15.81	17.62	17.20	19.27
160.0	20.44	19.85	15.81	15.15	17.34	17.82	19.38

TABLE 5.2 (i)

(for  $\text{CaCO}_3$ )Room Temperature :  $T_1 = 303^\circ\text{K}$ 

Load P in gm.	Hardness H in $\text{kg}\cdot\text{mm}^{-2}$						
	0 & 78°	7° & 70°	14° & 63°	21° & 56°	28° & 49°	35° & 42°	39°
1.25	105.17	185.2	158.07	146.57	170.96	185.96	136.29
2.5	137.67	196.2	174.45	184.87	184.87	196.24	156.10
3.75	150.57	210.75	181.73	190.69	190.69	210.75	165.58
5.0	167.14	220.78	185.51	193.49	193.49	211.07	170.96
6.25	173.45	205.41	183.22	176.61	176.61	205.43	158.13
7.5	175.16	197.33	184.17	161.53	161.53	204.44	151.74
8.75	179.24	194.58	182.61	161.76	161.76	201.01	148.39
10.0	162.99	184.87	174.45	160.41	151.97	174.45	133.56
11.25	157.26	170.96	175.61	166.49	150.26	154.09	121.41
12.5	152.34	162.86	166.96	155.11	147.89	155.10	109.02
13.75	150.31	151.78	162.68	155.29	148.39	124.92	106.61
15.0	150.67	139.13	148.25	151.52	148.25	116.30	105.97
16.25	142.88	138.91	144.63	136.17	150.72	114.80	103.23
17.5	143.31	133.14	146.64	135.68	141.00	113.14	102.17
18.75	139.99	132.46	145.38	134.90	137.41	111.30	94.84
20.0	138.04	131.55	141.29	124.89	129.27	96.65	87.22
30.0	136.08	130.84	149.43	128.99	130.84	88.73	82.79
40.0	131.38	125.59	131.91	116.96	133.56	96.75	86.34
50.0	125.35	125.88	131.91	117.16	123.54	101.70	96.00
60.0	124.46	123.24	128.22	122.04	110.95	105.97	101.31
70.0	117.36	118.2	128.45	118.20	113.16	105.64	97.29
80.0	120.39	118.72	128.15	127.05	114.86	97.38	97.38

TABLE 5.2 (ii)

(for  $\text{CaCO}_3$ )Quenching Temperature :  $T_{q1} = 498^\circ\text{K}$ 

Load P in gm.	Hardness H in $\text{kg-mm}^{-2}$					
	0 & $78^\circ$	$7^\circ$ & $70^\circ$	$14^\circ$ & $63^\circ$	$21^\circ$ & $56^\circ$	$28^\circ$ & $49^\circ$	$35^\circ$ & $42^\circ$
1.25	185.51	185.51	185.51	170.96	170.96	170.96
2.5	196.24	196.24	196.24	184.87	184.87	184.87
3.75	200.35	200.35	200.35	190.69	190.69	190.69
5.0	193.49	193.49	193.49	185.51	185.51	178.01
6.25	190.20	183.22	183.22	176.61	176.61	170.36
7.5	184.17	178.09	178.09	172.30	166.78	161.53
8.75	177.03	166.62	166.62	166.62	161.76	157.10
10.0	174.45	169.57	169.57	164.89	169.57	151.97
11.25	170.96	175.61	170.96	166.49	166.49	150.26
12.5	166.96	175.63	166.96	166.96	162.86	147.89
13.75	162.68	158.92	155.29	151.78	155.29	145.11
15.0	161.88	158.30	154.84	151.49	154.84	139.13
16.25	164.12	160.60	157.21	157.21	153.91	141.73
17.5	162.32	162.32	158.99	155.76	155.76	141.00
18.75	160.28	157.12	157.12	151.08	148.19	137.41
20.0	161.15	158.06	155.07	149.32	146.57	129.27
30.0	151.74	149.43	142.82	140.70	138.65	121.97
40.0	142.32	136.97	133.56	128.69	122.60	115.58
50.0	139.56	131.91	131.91	126.24	124.88	117.16
60.0	132.16	128.22	123.24	119.70	116.30	109.93
70.0	129.45	127.07	124.76	121.41	115.10	108.35
80.0	131.55	129.27	127.05	121.75	118.72	108.54

TABLE 5.2 (iii)

(for  $\text{CaCO}_3$ )

Quenching Temperature :  $T_{q2} = 573^\circ\text{K}$

Load P in gm.	Hardness H in $\text{kg-mm}^{-2}$					
	0 & $78^\circ$	$7^\circ$ & $70^\circ$	$14^\circ$ & $63^\circ$	$21^\circ$ & $56^\circ$	$28^\circ$ & $49^\circ$	$35^\circ$ & $42^\circ$
1.25	201.99	201.99	185.51	185.51	170.96	170.96
2.5	208.70	208.70	196.24	196.24	184.87	184.87
3.75	221.99	221.99	210.75	210.75	210.75	200.35
5.0	201.99	201.99	201.99	193.49	193.49	185.51
6.25	197.58	190.20	190.20	183.22	184.22	176.61
7.5	190.58	184.17	184.17	178.09	172.30	166.78
8.75	182.61	177.03	177.03	171.71	171.71	161.76
10.0	179.55	174.45	174.45	169.57	169.57	156.10
11.25	175.61	170.96	170.96	170.96	166.49	154.09
12.5	171.21	162.86	162.86	171.21	166.96	155.10
13.75	166.58	162.68	162.68	158.92	155.29	148.39
15.0	169.40	161.88	165.58	161.88	148.25	142.07
16.25	171.49	167.74	164.12	160.60	157.21	149.08
17.5	169.30	165.75	162.32	158.99	158.99	149.59
18.75	166.89	163.53	160.28	157.12	154.05	139.99
20.0	167.59	164.32	161.15	158.06	155.07	133.89
30.0	156.52	151.74	144.97	142.82	140.71	123.67
40.0	146.07	142.32	140.50	135.25	125.59	122.60
50.0	139.56	136.42	134.90	133.39	129.03	119.65
60.0	134.88	133.51	130.82	129.51	122.04	113.05
70.0	135.68	129.45	127.07	125.91	123.63	113.11
80.0	135.08	131.55	128.15	123.83	123.83	118.72

TABLE 5.2 (iv)

(for  $\text{CaCO}_3$ )Quenching Temperature :  $T_{q3} = 698^\circ\text{K}$ 

Load P in gm.	Hardness H in $\text{kg-mm}^{-2}$					
	0 & 78°	7° & 70°	14° & 63°	21° & 56°	28° & 49°	35° & 42°
1.25	220.77	220.77	220.77	201.99	201.99	201.99
2.5	222.38	222.38	222.38	208.70	208.70	208.70
3.75	210.75	210.75	200.35	190.69	190.69	181.72
5.0	201.99	201.99	193.49	193.49	185.51	185.51
6.25	213.70	205.41	205.41	197.58	190.20	183.22
7.5	204.44	204.44	197.33	197.33	190.58	184.17
8.75	188.45	188.45	182.61	182.61	177.03	171.71
10.0	190.42	190.42	184.87	179.55	174.45	169.57
11.25	185.51	180.46	175.61	170.96	166.49	162.20
12.5	180.22	180.22	175.63	175.63	171.21	166.96
13.75	170.62	170.62	166.58	166.58	162.68	158.92
15.0	177.47	173.37	169.40	161.88	158.30	151.49
16.25	175.37	167.74	160.60	157.21	153.91	150.72
17.5	172.96	169.30	162.32	158.99	155.76	152.63
18.75	170.35	166.89	160.28	154.05	148.19	145.38
20.0	170.96	164.32	158.06	152.16	146.57	141.29
30.0	161.53	156.52	151.74	144.97	138.65	130.84
40.0	149.96	146.07	144.17	138.72	136.97	131.91
50.0	142.81	139.56	133.39	129.03	124.88	122.22
60.0	140.59	133.51	128.22	123.24	118.55	116.30
70.0	134.40	131.89	129.45	125.91	121.41	119.25
80.0	138.76	135.08	132.71	127.05	128.15	123.83

TABLE 5.2 (v)

(for  $\text{CaCO}_3$ )Quenching Temperature :  $T_{q4} = 773^\circ\text{K}$ 

Load P in gm.	Hardness H in $\text{kg}\cdot\text{mm}^{-2}$					
	0 & $78^\circ$	$7^\circ$ & $70^\circ$	$14^\circ$ & $63^\circ$	$21^\circ$ & $56^\circ$	$28^\circ$ & $49^\circ$	$35^\circ$ & $42^\circ$
1.25	220.77	220.77	220.77	201.99	201.99	201.99
2.5	237.45	237.45	237.45	222.38	222.38	222.38
3.75	221.99	234.15	221.99	221.99	221.99	210.75
5.0	211.07	211.07	211.07	201.99	201.99	193.49
6.25	205.41	205.41	205.41	197.58	197.58	190.20
7.5	197.33	197.33	190.58	190.58	184.17	178.09
8.75	194.58	194.58	188.45	182.61	182.61	177.03
10.0	190.42	190.42	184.87	179.55	179.55	174.45
11.25	190.77	185.51	180.46	175.61	170.96	166.49
12.5	184.99	180.22	175.63	171.21	160.96	162.86
13.75	174.80	174.80	170.62	166.58	162.68	162.68
15.0	181.72	177.47	169.40	161.88	158.30	154.84
16.25	179.37	171.49	167.74	164.12	160.60	153.91
17.5	176.74	172.96	169.30	162.32	158.99	155.76
18.75	177.59	170.35	163.53	157.12	154.05	148.19
20.0	174.43	167.59	161.15	155.07	149.32	146.57
30.0	159.00	154.10	149.43	144.97	140.71	134.66
40.0	151.97	146.07	138.72	135.25	131.91	128.69
50.0	147.89	142.81	139.56	133.39	130.46	124.88
60.0	142.07	139.13	134.88	130.82	128.22	122.04
70.0	142.38	139.65	135.68	131.89	125.91	121.41
80.0	141.29	137.51	133.89	128.15	124.89	121.75

TABLE 5.3 (a)

Mean hardness values  $\bar{H}$  in  $\text{Kg-mm}^{-2}$  of H Vs. P  
*from plots*  
 (Fig.5.1) for  $\text{NaNO}_3$  (Applied loads  $> 20$  gm.)

Orientation A in degrees	Temperature T				
	298°K	343°K	393°K	443°K	493°K
0	22.63	22.91	20.18	20.99	21.47
13	20.93	20.4	18.11	19.62	20.63
26	17.94	18.31	17.18	16.53	16.98
39	17.40	19.29	16.63	16.28	16.36
52	17.46	18.19	17.16	16.64	17.83
65	18.89	21.07	19.34	19.30	17.93
78	22.27	22.12	20.30	20.16	19.97

TABLE 5.3 (b)

Calculation of H by using relation

$$H = 14230.a^{2/n}.P^{(n-2)/n} \text{ (for NaNO}_3\text{)}$$

$$P = 100 \text{ gm.}$$

Orientation A in degrees	Temperature T				
	298°K	343°K	393°K	443°K	493°K
0	23.18	23.37	19.98	20.04	21.28
13	19.95	20.52	18.29	20.94	20.02
26	16.49	17.86	17.50	16.33	24.23
39	15.58	19.54	16.21	16.15	15.97
52	14.33	18.00	16.76	16.13	17.44
65	18.19	19.89	19.96	20.05	19.03
78	21.35	21.71	19.18	20.06	20.86

TABLE 5:3 (C)

Calculation of  $H$  by using relation

$$H = 14230 \cdot b \quad (\text{for NaNO}_3)$$

Orientation A in degrees	Temperature T				
	298°K	343°K	393°K	443°K	493°K
0	21.82	21.77	19.38	18.72	20.03
13	18.21	18.39	17.10	20.17	18.88
26	15.08	16.56	16.76	15.08	22.30
39	14.23	18.09	15.16	15.19	15.14
52	13.19	16.55	15.96	14.71	16.75
65	16.45	18.16	19.45	18.72	18.49
78	19.77	15.72	18.45	19.05	20.27

TABLE 5.3 D(i)

Percentage deviation of calculated H by using relation

$$H = 14230 \cdot a^{2/n} \cdot p^{(n-2)/n}$$

from the observed graphical value (for  $\text{NaNO}_3$ )

Orientation A in degrees	Temperature T				
	298°K	343°K	393°K	443°K	493°K
0	2.43	2.01	-0.99	-4.53	-0.88
13	-4.68	0.59	0.99	6.73	-2.96
26	-8.08	-2.46	1.86	-1.21	-12.70
39	-10.45	1.19	-2.53	-0.79	-2.38
52	-17.93	-1.04	-2.33	-3.06	-2.19
65	-3.71	-5.60	0.60	3.89	6.16
78	-4.13	-1.85	-5.52	-0.49	4.46

TABLE 5.3 D(ii)

Percentage deviation of calculated H by using relation,

$$H = 14230 . b$$

from the observed graphical value (for  $\text{NaNO}_3$ )

Orientation A in degrees	Temperature T				
	298°K	343°K	393°K	443°K	493°K
0	- 3.57	- 4.98	- 3.96	- 10.81	- 6.71
13	- 12.99	- 9.85	- 5.58	2.80	- 8.48
26	- 15.94	- 9.56	- 2.44	- 8.77	13.33
39	- 18.21	- 6.22	- 8.84	- 6.69	- 7.45
52	- 24.45	- 9.02	- 6.99	- 11.59	- 6.06
65	- 12.92	- 13.81	- 1.97	- 3.01	3.12
78	- 20.21	- 28.93	9.11	- 5.51	1.50

TABLE 5.4 (A)

from plots

Mean hardness values  $\bar{H}$  in  $\text{kg-mm}^{-2}$  of H Vs. P (Fig.5.2)  
for  $\text{CaCO}_3$  (Applied loads  $>$  40 gm.)

Orientation A in degrees	Temperature T				
	303°K	498°K	573°K	698°K	773°K
0	123.78	135.00	138.25	141.30	145.12
7	122.12	130.69	135.43	137.22	141.03
14	129.92	128.10	132.29	133.59	136.55
21	120.28	123.56	124.58	128.78	131.90
28	119.21	119.52	124.82	125.99	128.27
35	101.49	111.91	117.43	122.70	123.75

TABLE 5.4 (B)

Calculation of H by using relation,

$$H = 14230 \cdot a_2^{2/n_2} \cdot P^{(n_2-2)/n_2}$$

(for  $\text{CaCO}_3$ )

$$P = 50 \text{ gm}$$

Orientation A in degrees	Temperature T				
	303°K	498°K	573°K	698°K	773°K
0	116.17	118.83	131.07	133.33	147.65
7	129.11	118.83	123.77	130.30	135.53
14	135.11	118.83	119.96	130.30	130.30
21	112.04	107.26	116.94	119.30	119.30
28	113.15	118.2	121.96	127.25	127.25
35	84.93	105.83	113.53	113.53	116.17

TABLE 5.4 (C)

Calculation of H by using relation,

$$H = 14230 \cdot b \quad (\text{for CaCO}_3)$$

Orientation A in degrees	Temperature T				
	303°K	498°K	573°K	698°K	773°K
0	99.61	103.16	112.52	112.41	127.64
7	106.68	102.95	106.79	111.84	116.30
14	119.07	102.44	102.45	111.56	111.56
21	96.33	91.17	99.18	100.32	100.69
28	96.76	101.87	106.44	110.14	109.94
35	99.46	89.78	97.09	97.76	99.73

TABLE 5.4 D(i)

Percentage deviation of calculated H by using relation,

$$H = 14230 \cdot a_{\perp}^{2/n_{\perp}} \cdot P^{(n_{\perp}^2)/n_{\perp}}$$

from the observed graphical value for  $\text{CaCO}_3$

Orientation A in degrees	Temperature T				
	303°K	498°K	573°K	698°K	773°K
0	-6.15	-11.98	-5.19	-5.64	1.74
7	5.72	-9.07	-8.61	-5.04	-3.89
14	3.99	-7.24	-9.32	-2.46	-4.58
21	-6.85	-9.32	-9.75	-7.36	-9.55
28	-5.08	-1.10	-2.29	1.00	-0.71
35	-16.32	-5.43	-3.32	-7.47	-6.13

TABLE 5.4 D(ii)

Percentage deviation of calculated H by using relation,

$$H = 14230 \cdot b_2$$

from the observed graphical value for  $\text{CaCO}_3$

Orientation A in degrees	Temperature T				
	303°K	498°K	573°K	698°K	773°K
0	-19.52	-23.58	-18.61	-20.45	-12.04
7	-12.64	-21.23	-21.15	-18.49	-17.53
14	-8.35	-20.03	-22.56	-16.49	-18.30
21	-19.91	-26.21	-23.46	-22.09	-23.66
28	-18.83	-14.77	14.73	-12.58	-14.29
35	-2.00	-19.77	-17.33	-20.32	-19.41

TABLE 5.5

Angle :  $0^\circ$ 

Temp : 298°K

W : 1.198

P in gm	d in $\mu$	P - W	H in $\text{kg-mm}^{-2}$	$H=14230 \frac{P-W}{d^2}$
1.25	22.8	0.052	34.07	1.423
2.5	33.5	1.302	31.78	16.509
3.75	43.2	2.552	28.53	19.45
5.0	49.8	3.802	28.71	21.81
6.25	56.3	5.052	28.05	21.680
7.5	64.5	6.302	25.68	21.555
8.75	68.5	7.552	26.50	22.90
10.0	73.4	8.802	26.38	23.248
11.25	77.5	10.052	26.64	23.815
12.5	81.6	11.302	26.71	24.15
13.75	85.7	12.552	26.65	24.319
15.0	93.8	13.802	24.23	22.32
16.25	96.3	15.052	24.94	23.096
17.5	99.6	16.302	25.12	23.384
18.75	102.8	17.552	25.24	23.63
20.0	108.5	18.802	24.16	22.727
25.0	120.2	23.802	24.39	23.44
30.0	134.6	28.802	23.54	22.62
40.0	156.7	38.802	23.18	22.48
50.0	175.4	48.802	23.12	22.57
60.0	195.0	58.802	22.44	22.005
70.0	209.7	68.802	22.64	22.24
80.0	226.8	78.802	22.122	21.79
100.0	257.0	78.802	21.54	21.28
120.0	279.0	118.802	21.79	21.57
140.0	306.0	138.802	21.28	21.09
160.0	326.4	158.802	21.37	21.211

 $\bar{H} = 22.63, 22.085$ 

2.466% variation in mean value

TABLE 5.6

Table 5.6(A)

Knoop hardness values obtained from the plot of H Vs. P, from equation (5.8) & (5.9) for  $\text{NaNO}_3^*$

Temp °K	Knoop Hardness numbers, $\text{kg-mm}^{-2}$		
	from graph $H_K=14230 P/d^2$	$H_K=14230 a^{2/n} \cdot P^{(n-2)/n}$	$H_K=14230 b_2$
303	18.89	18.89	66.88
373	18.82	18.82	74.88
398	18.89	18.89	75.18
423	19.14	19.14	78.43
448	19.51	19.51	76.98
473	19.95	19.95	81.69
498	20.01	20.01	81.32
533	20.44	20.44	86.24

Table 5.6(B)

Vickers hardness values obtained from the plot of H Vs. P, from equation (5.8) & (5.9) for  $\text{NaNO}_3^*$

Temp °K	Vickers Hardness numbers, $\text{kg-mm}^{-2}$		
	from graph $H_V=1854.4 P/d^2$	$H_V=1854.4 a^{2/n} \cdot P^{(n-2)/n}$	$H_V=1854.4 b_2$
303	18.75	17.46	47.68
373	18.95	17.54	49.81
398	19.30	17.46	50.7
423	19.42	19.06	50.42
448	19.71	19.14	51.37
473	19.71	19.26	50.24
498	19.96	19.35	50.74
533	20.09	19.81	49.75

\* The values from the plot H Vs. P is taken from the Ph.D. Thesis of Dr. A.J. Shah.

TABLE 5.7

For  $\text{NaNO}_3$  crystals

log $T_q$	log $\bar{H} T_q$						
	A = 0°	A = 13°	A = 26°	A = 39°	A = 52°	A = 65°	A = 78°
2.4742	3.8289	3.7949	3.7280	3.7147	3.7162	3.7504	3.8219
2.5352	3.8953	3.8449	3.7979	3.8206	3.7951	3.8589	3.8801
2.5943	3.8993	3.8523	3.8294	3.8152	3.8289	3.8919	3.9018
2.6464	3.9684	3.9391	3.8646	3.8581	3.8676	3.9319	3.9509
2.6928	4.0246	4.0073	3.9226	3.9066	3.9439	3.9464	3.9932
Slope(m)	0.811	0.825	0.838	0.875	0.85	0.818	0.804
C	66.95	57.21	45.43	35.53	43.15	59.07	68.11
K= 1-m	0.189	0.175	0.162	0.125	0.150	0.182	0.196

**TABLE 5.8**  
for  $\text{CaCO}_3$  crystal

Log $T_q$	Log $\bar{H} T_q$					
	A = 0°	A = 7°	A = 14°	A = 21°	A = 28°	A = 35°
2.4814	4.5741	4.5682	4.5951	4.5616	4.5577	4.4878
2.6946	4.8249	4.8108	4.8021	4.7864	4.7720	4.7435
2.7581	4.8988	4.8898	4.8796	4.8706	4.8544	4.8279
2.8438	4.9939	4.9812	4.9696	4.9510	4.9441	4.9327
2.8882	5.0499	5.0375	5.0235	5.0084	4.9963	4.9807
Slope (m)	1.15	1.09	1.04	1.09	1.12	1.21
C	51.28	73.77	102.99	68.45	75.30	30.52
K = 1 - m	-0.15	-0.09	-0.04	-0.09	-0.12	-0.21

TABLE 5.9

Values from the plot of  $\log T_q d$  Vs.  $\log T_q$   
for  $\text{NaNO}_3$  crystal at angle =  $0^\circ$

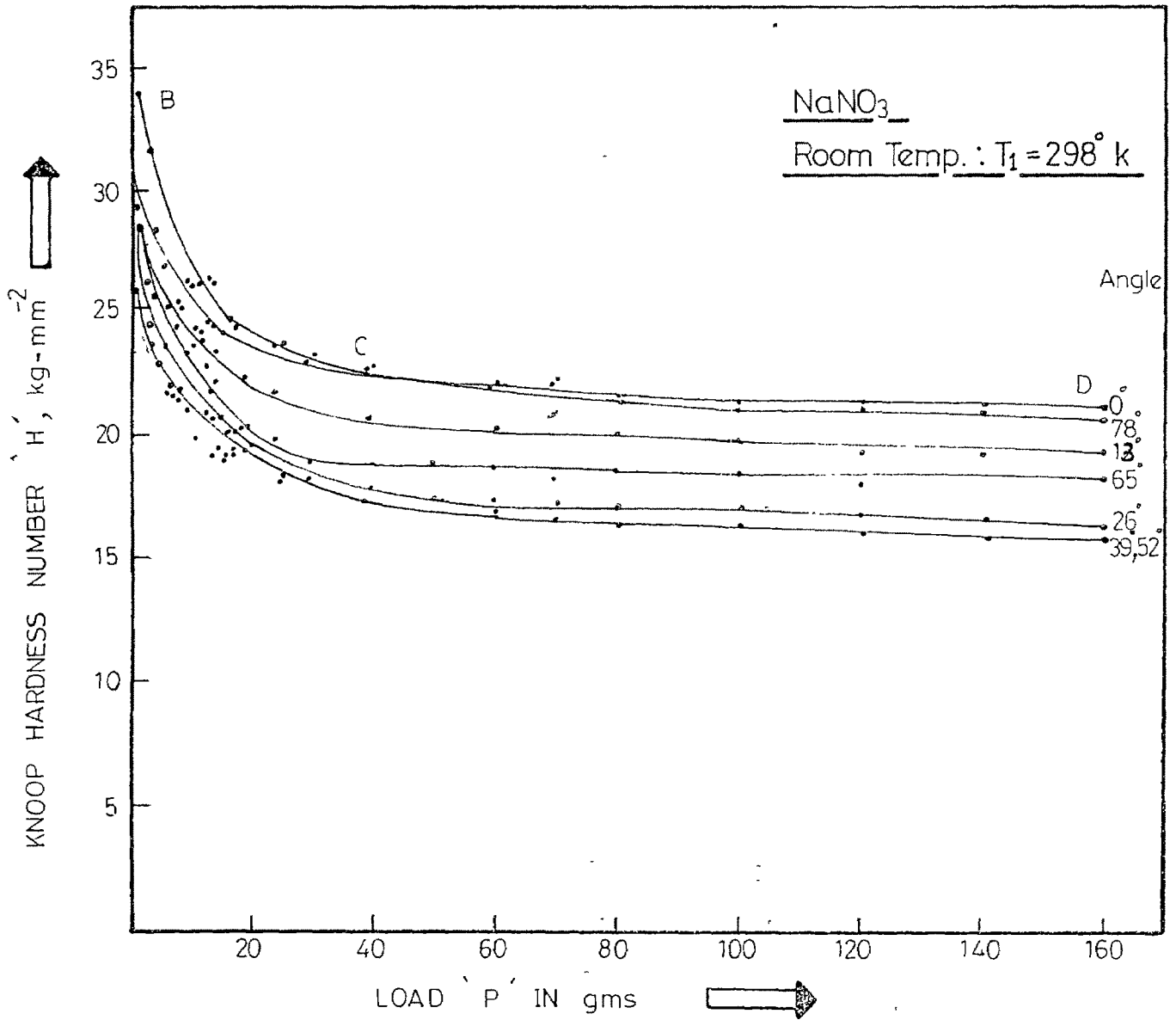
Load P in gm	Slope $m_{Ar}$	LHS = RHS $\frac{C_{Ar}}{\sqrt{P_r}} = \sqrt{\frac{14230}{C_A}}$ = 14.57	% variation in LHS & RHS
		LHS	
20	1.063	16.97	16
30	1.116	12.71	12
40	1.112	13.06	10
50	1.076	16.08	10
60	1.091	14.92	2
70	1.088	15.07	3
120	1.089	15.34	5
140	1.094	14.83	2
160	1.069	17.33	18

$\bar{m}_{Ar} = 1.0908$

Value of  $C_A$  is taken from the plots of  $\log \bar{H} T_q$  Vs.  $\log T_q$  which is equal to 66.95

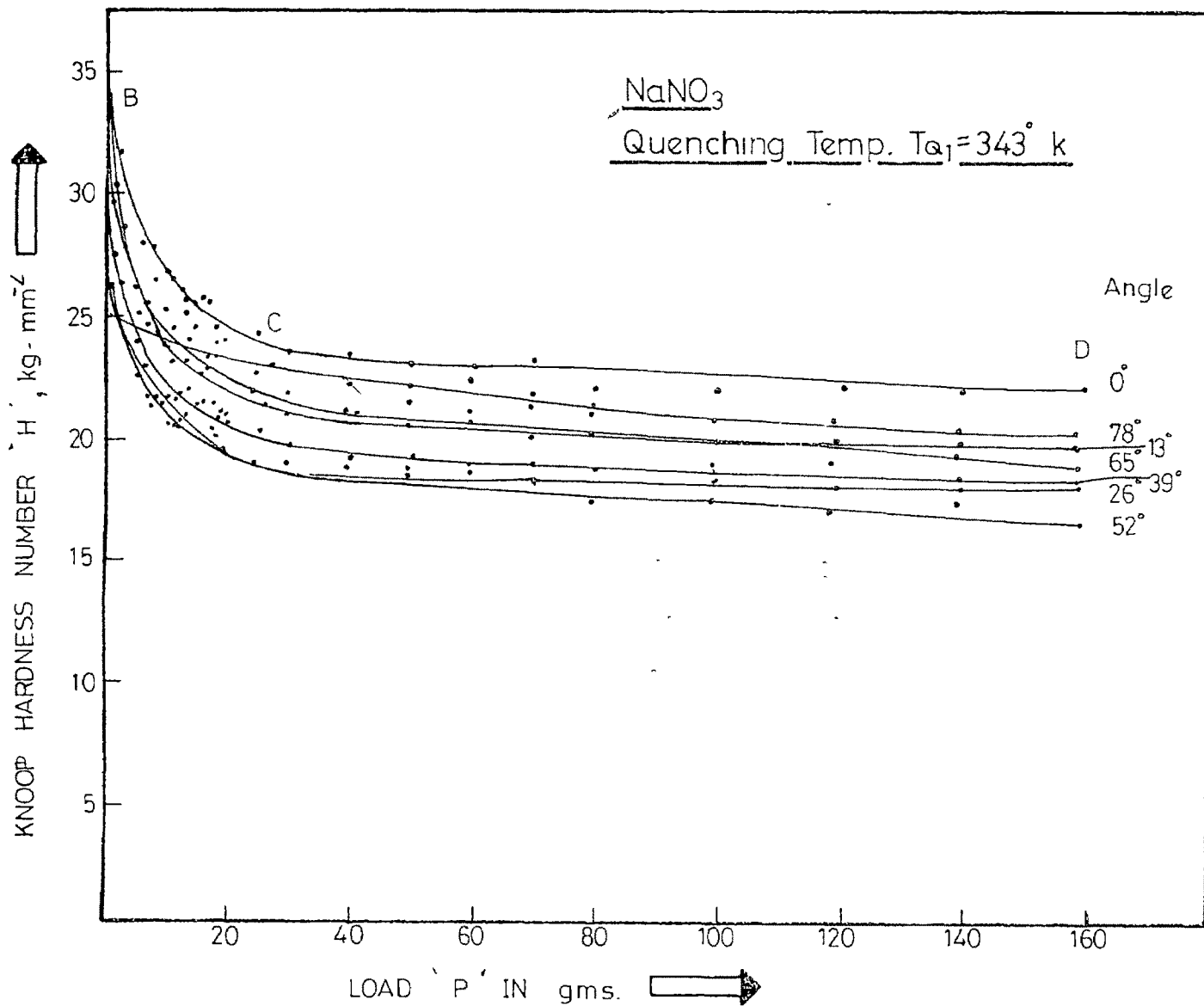
TABLE 5.10

NaNO <sub>3</sub>		Temp T°K	298	343	393	443	493			
Orientation A°	Load P in gm	diagonal length of Knoop indentation mark d in μ					C <sub>A</sub>	K <sub>A</sub>		
0°	40	156.67	155.86	165.65	164.83	163.20	66.95	0.189		
	60	195.02	192.58	206.45	201.55	201.55				
	100	257.04	252.14	267.65	261.12	261.12				
	140	306.0	301.92	318.24	311.71	311.71				
13°	40	164.83	164.83	167.28	168.91	165.65	57.21	0.175		
	60	203.18	204.00	208.89	210.52	203.18				
	100	265.2	269.28	271.73	269.28	263.57				
	140	318.24	318.24	322.32	323.13	319.05				
26°	40	177.07	174.62	181.97	183.60	178.70	45.43	0.162		
	60	221.14	214.61	223.58	227.60	228.48				
	100	287.23	280.70	294.58	296.20	293.76				
	140	342.72	337.00	349.25	357.40	353.32				
39°	40	172.99	171.36	179.52	185.23	184.41	35.53	0.125		
	60	223.58	211.34	235.01	233.37	233.37				
	100	295.39	275.81	296.21	297.84	297.84				
	140	34.43	326.4	350.88	354.96	354.96				
52°	40	178.70	172.18	176.26	181.97	179.52	43.15	0.15		
	60	219.50	212.98	222.77	224.40	220.32				
	100	288.86	286.42	292.94	289.68	283.96				
	140	345.98	337.82	354.96	350.88	336.19				
65°	40	172.18	159.12	168.91	169.73	179.52	59.07	0.182		
	60	212.98	199.92	206.45	212.16	224.40				
	100	276.62	271.73	271.73	276.99	285.60				
	140	341.09	316.61	320.69	326.40	340.27				
78°	40	158.30	159.12	167.28	167.28	167.28	68.11	0.198		
	60	196.66	194.21	204.00	205.63	208.08				
	100	258.67	260.30	265.20	266.01	269.28				
	140	307.63	315.79	320.69	322.32	321.50				



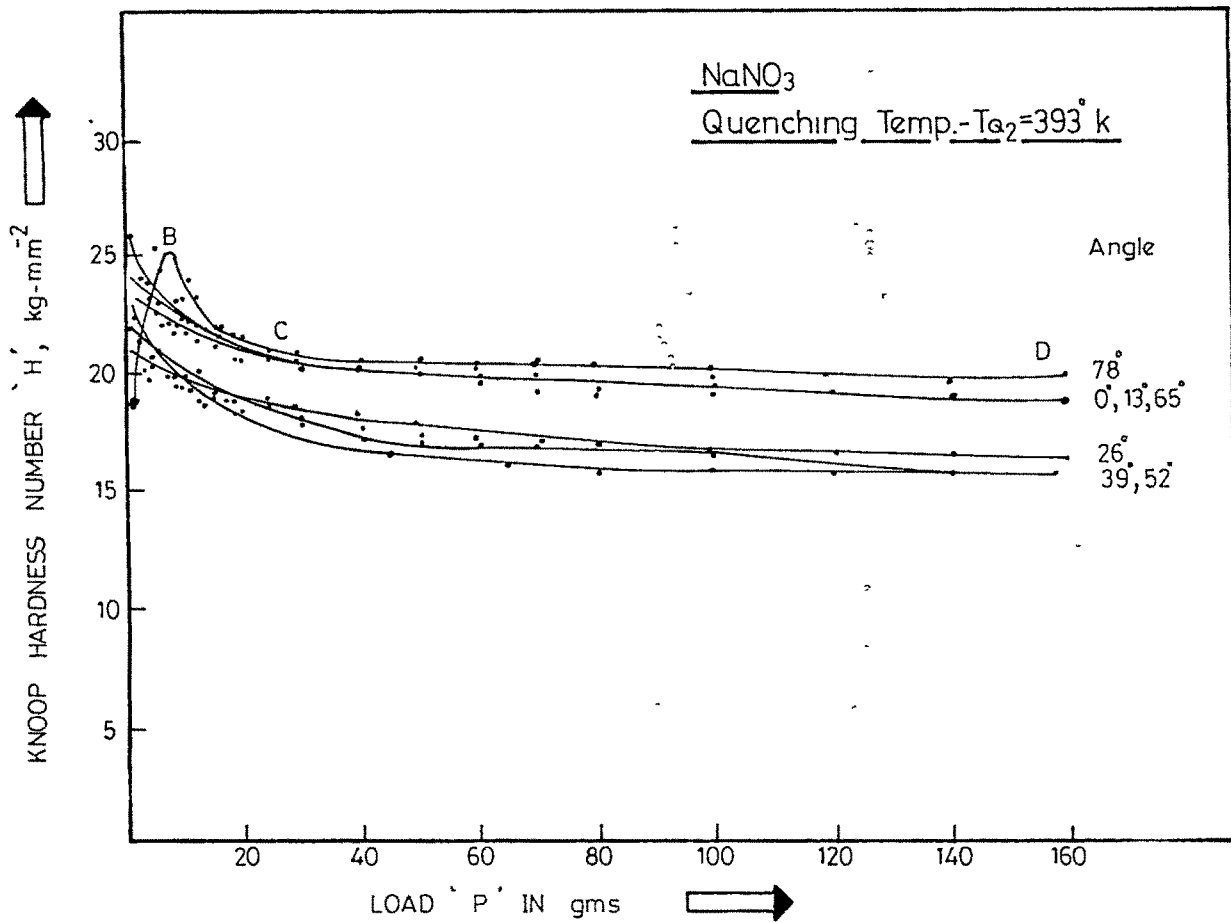
PLOT OF KNOOP HARDNESS NUMBER vs LOAD.

Fig.: 5.1 (I)



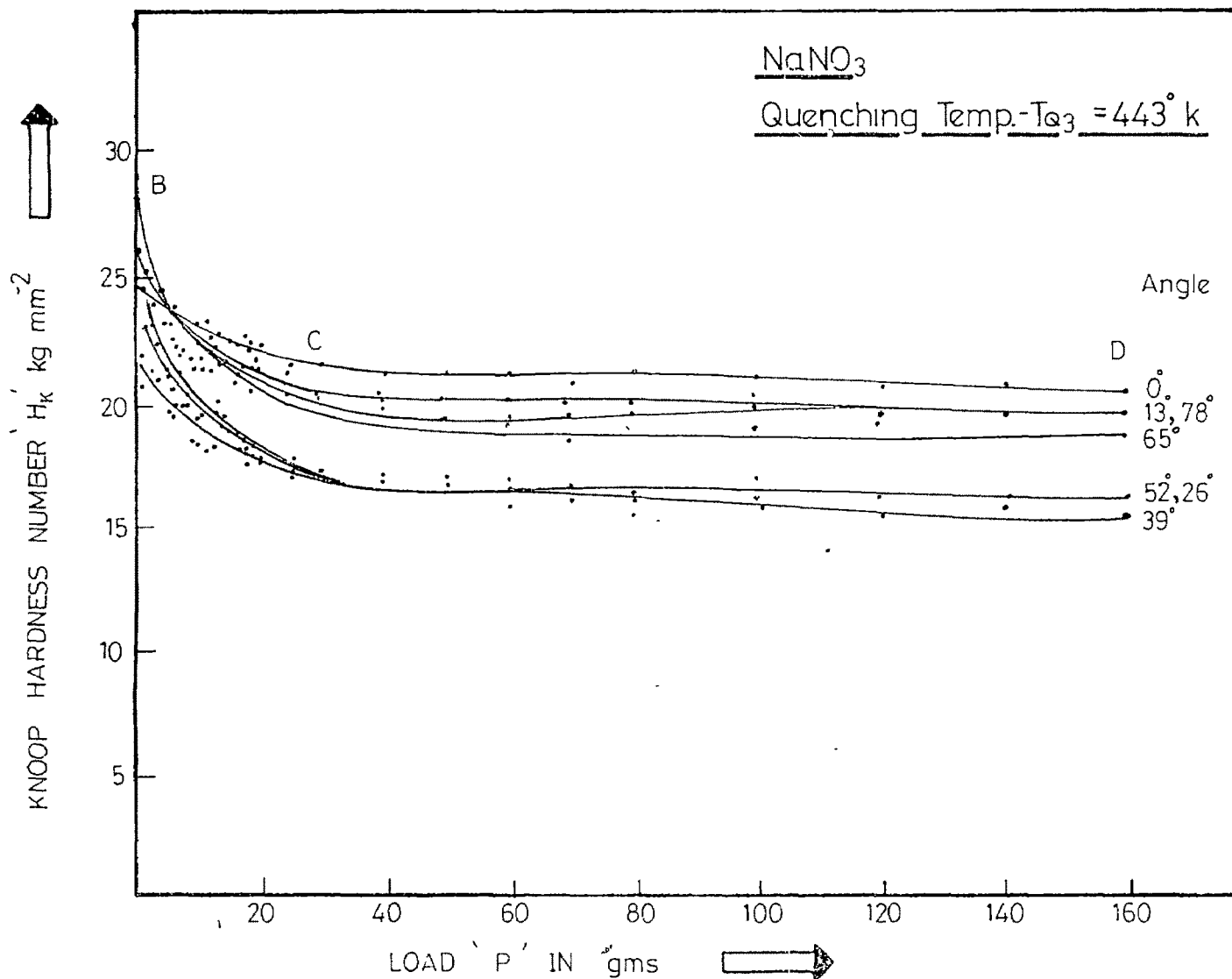
PLOT OF KNOOP HARDNESS NUMBER vs LOAD.

Fig. 5.1 (II)



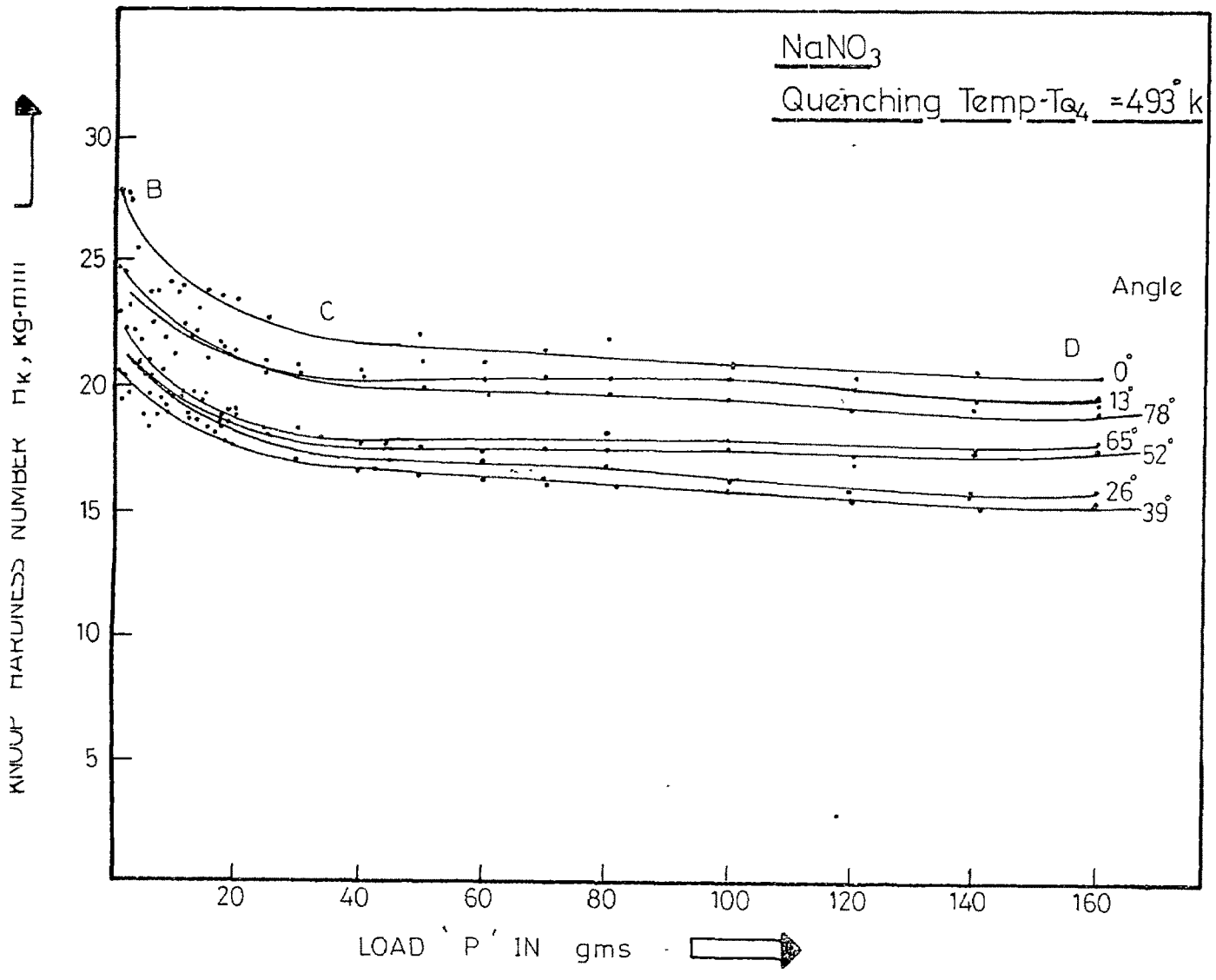
PLOT OF KNOOP HARDNESS NUMBER vs LOAD

Fig: 5-1 (III)



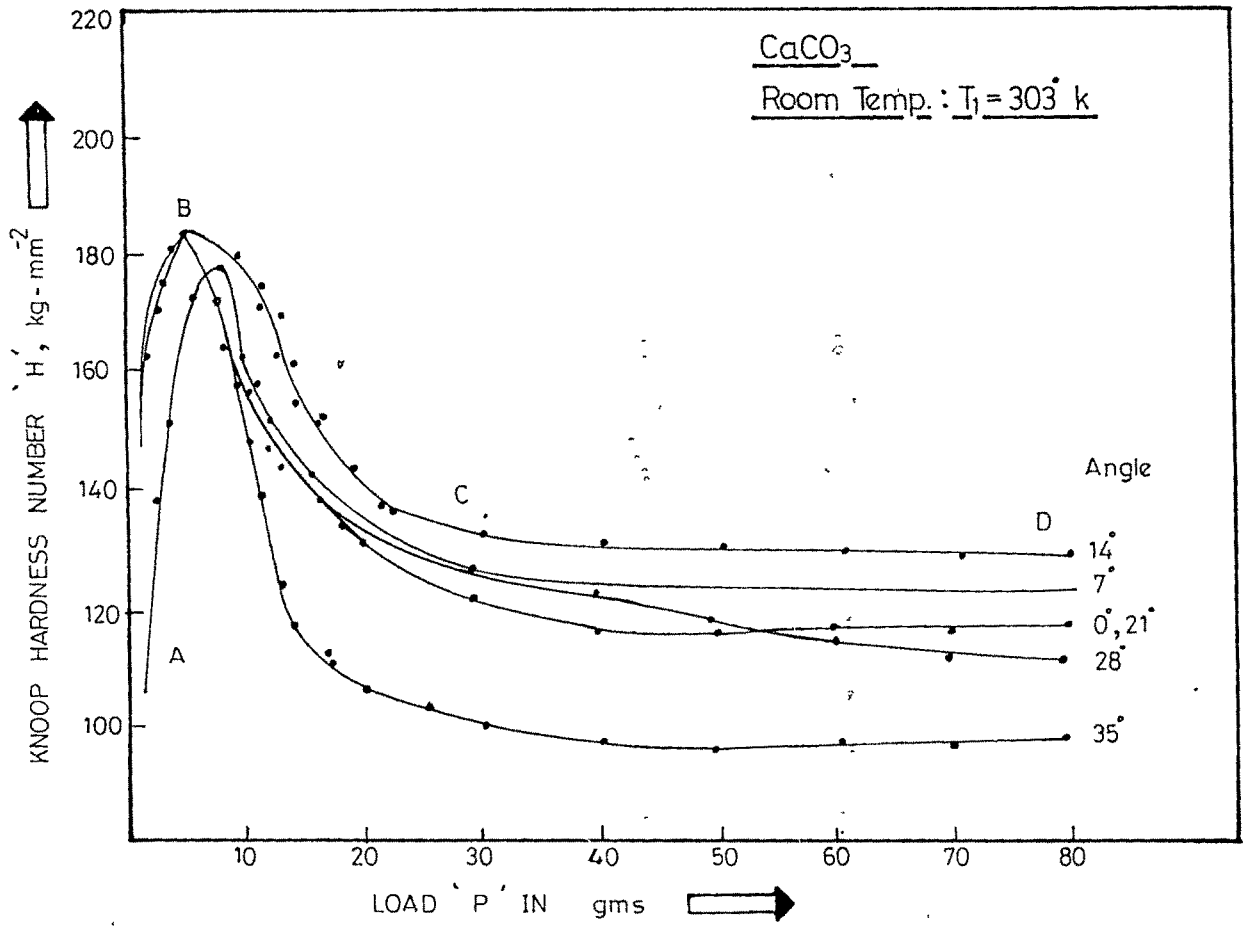
PLOT OF KNOOP HARDNESS NUMBER vs LOAD

Fig.: 5.1 (IV)



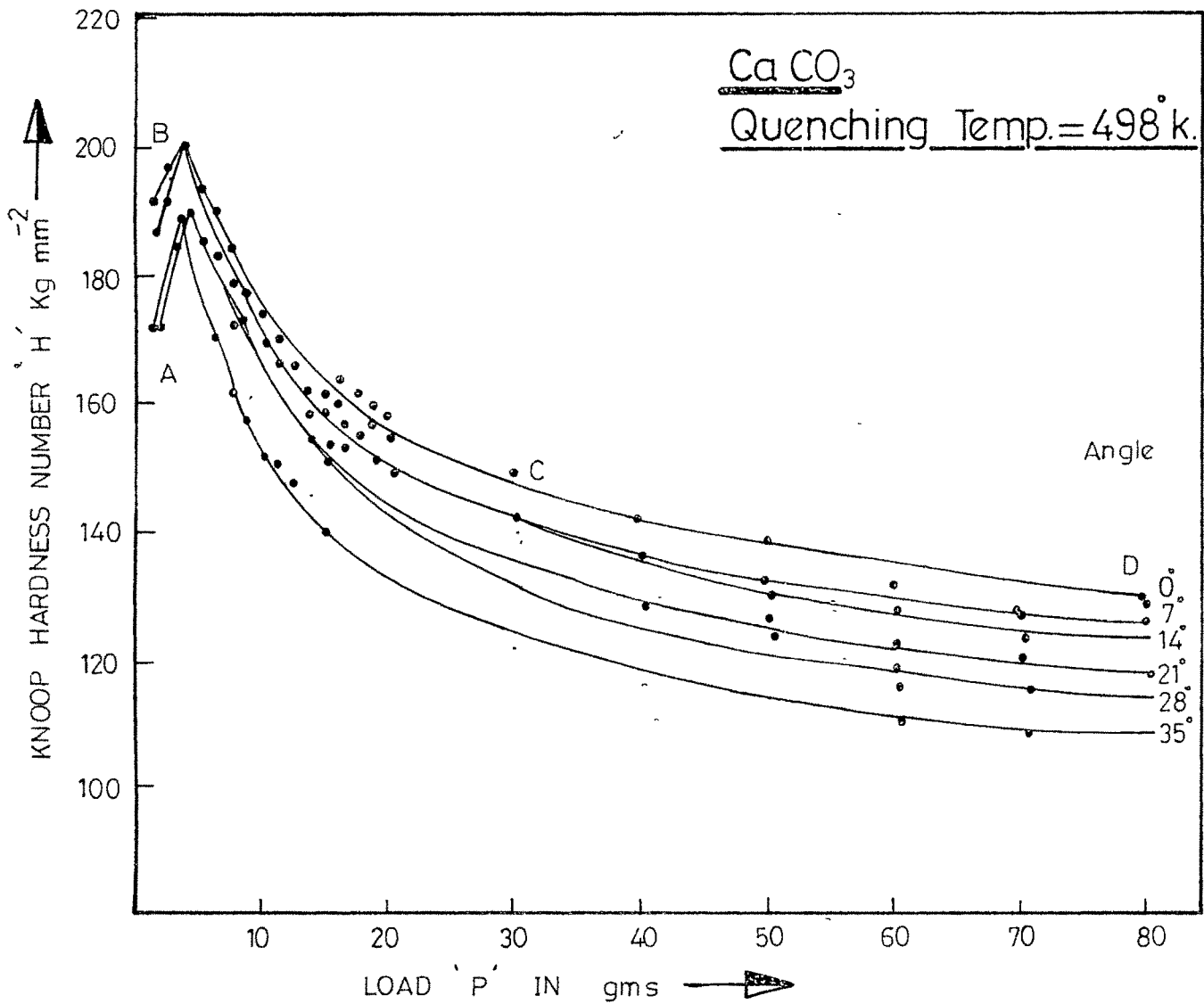
PLOT OF KNOOP HARDNESS NUMBER vs LOAD.

Fig.: 5.1(V)



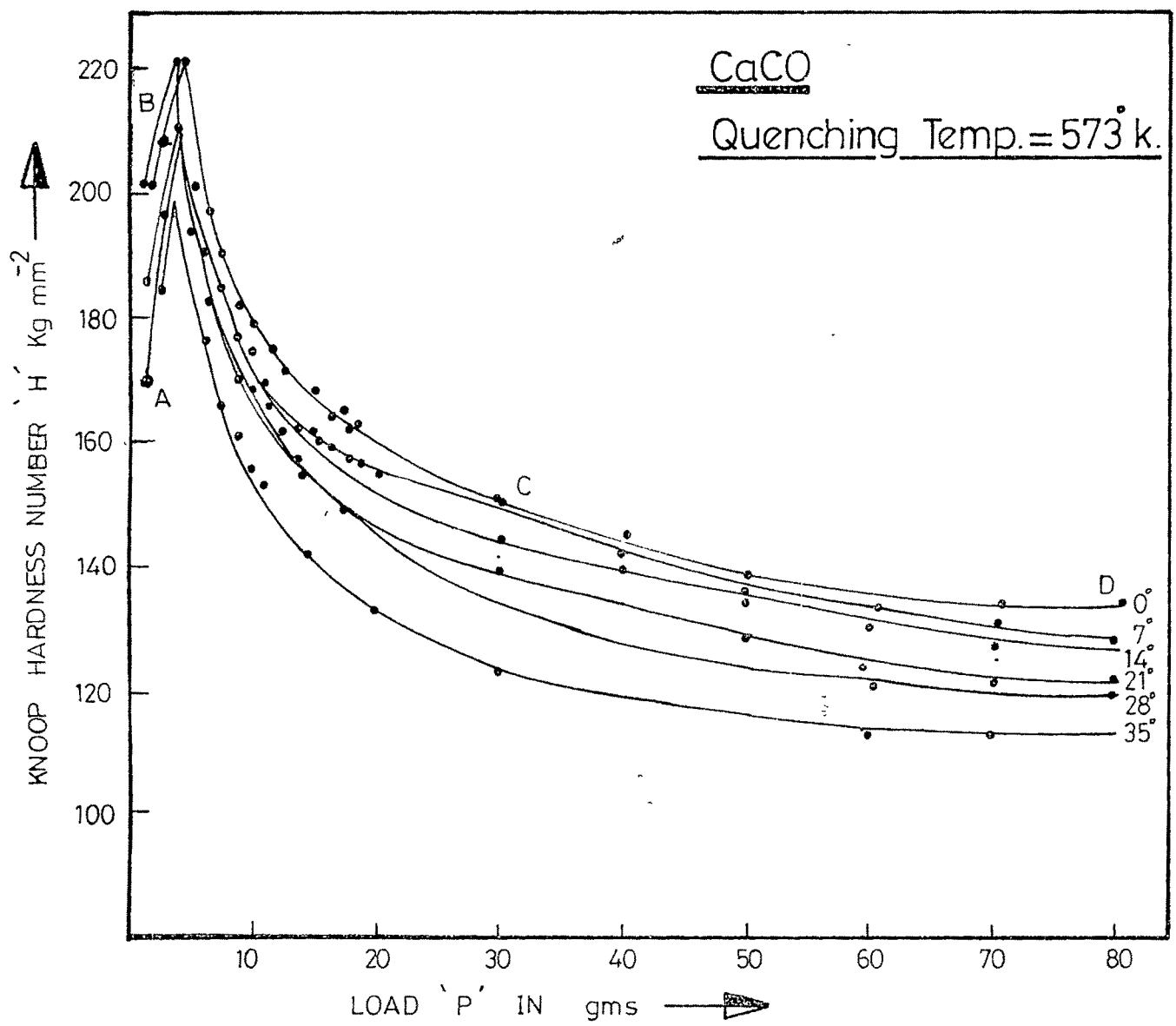
Plot of Knoop hardness number 'H' vs Load 'P'.

Fig.: 5.2 (I)



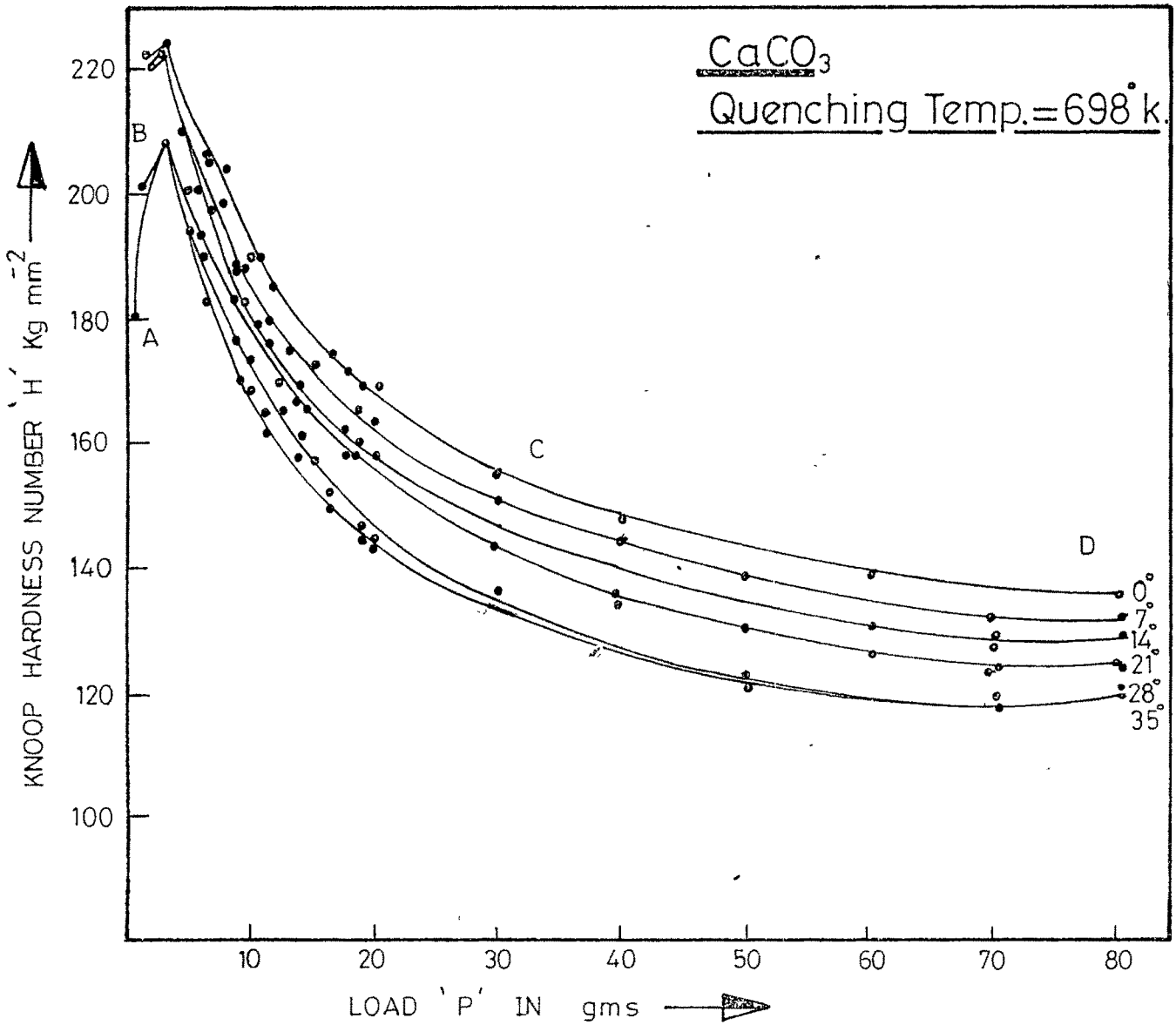
Plot of knoop hardness number 'H' vs Load 'P'

Fig: 5·2 (II)



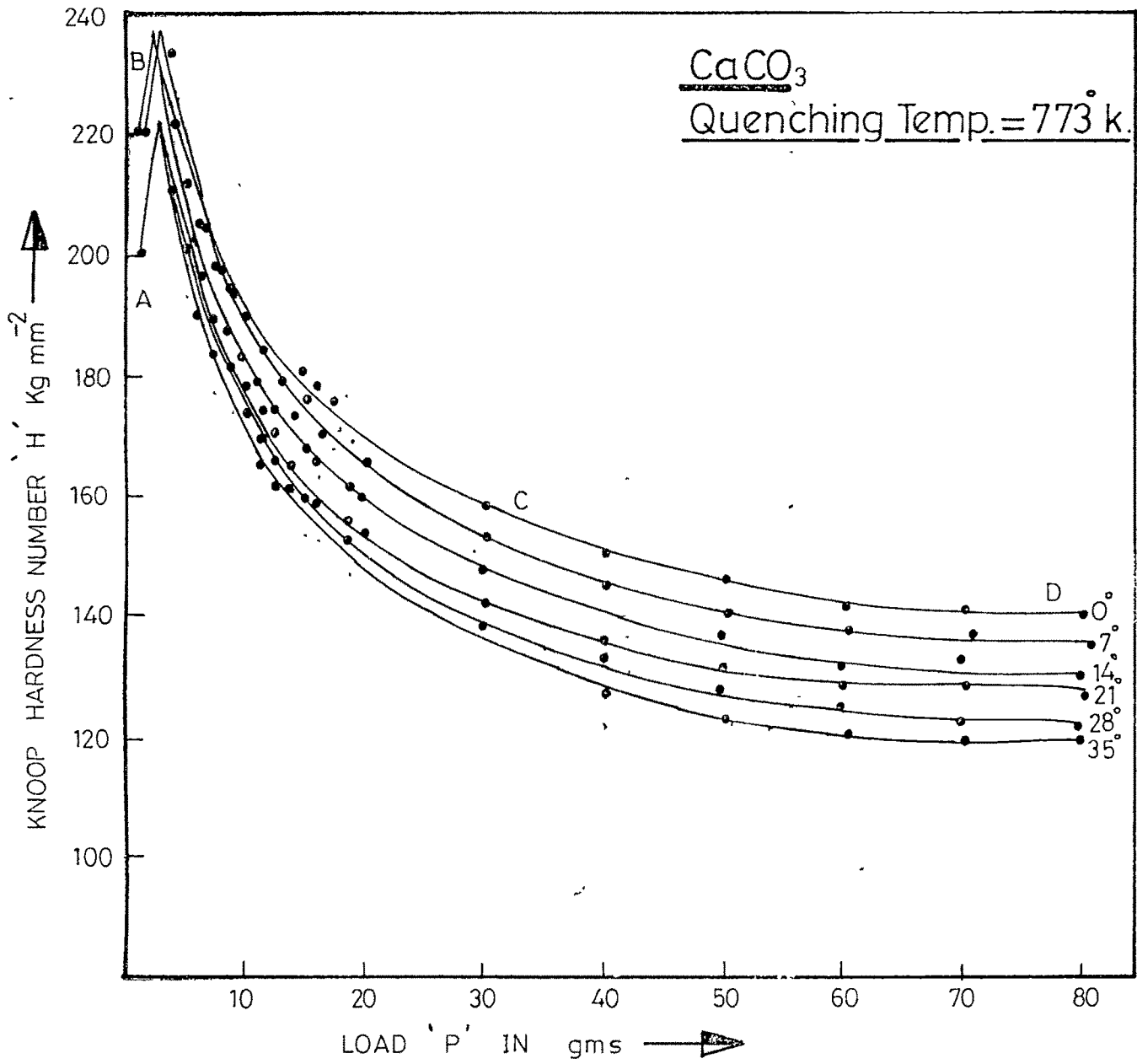
Plot of knoop hardness number 'H' vs Load 'P'

Fig: 5.2(III)



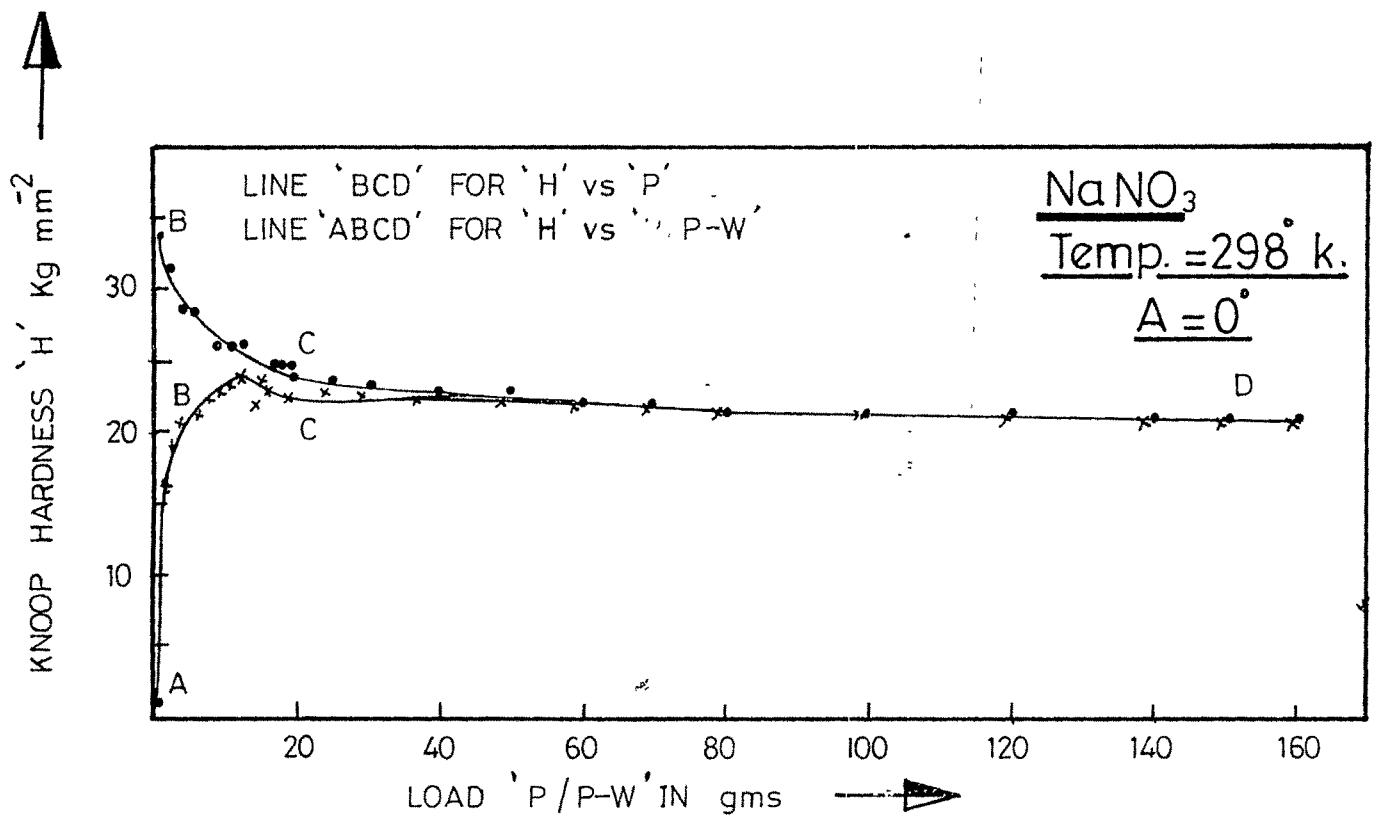
Plot of knoop hardness number 'H' vs Load 'P'

Fig: 5.2 (IV)



Plot of knoop hardness number 'H' vs Load 'P'

Fig: 5.2 (V)



Plot of 'H' vs 'P/P-W'

Fig: 5-3

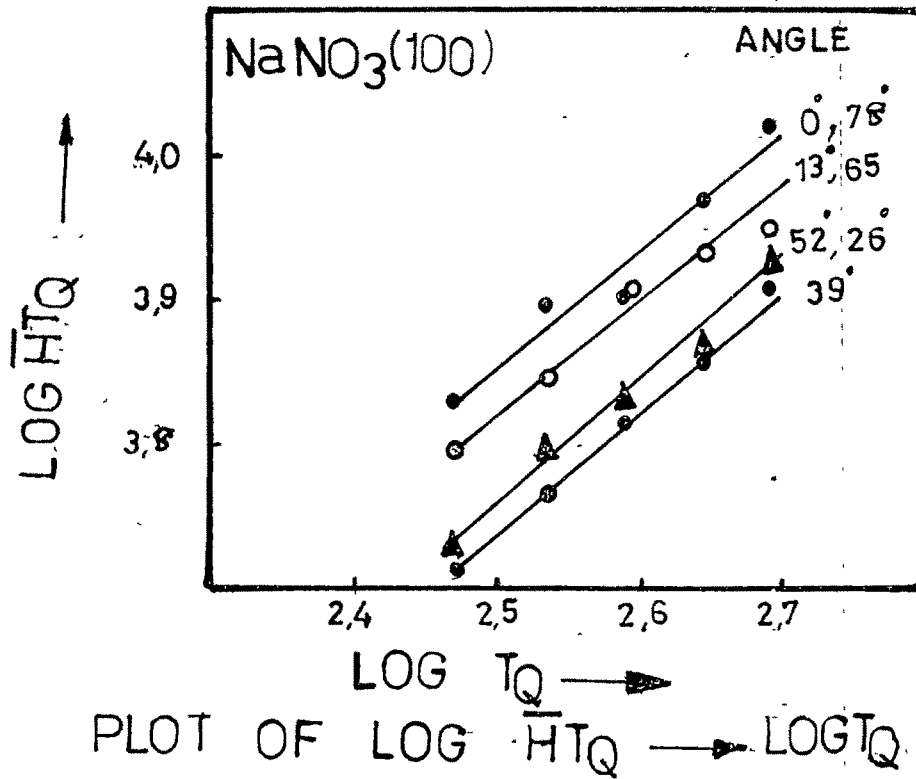
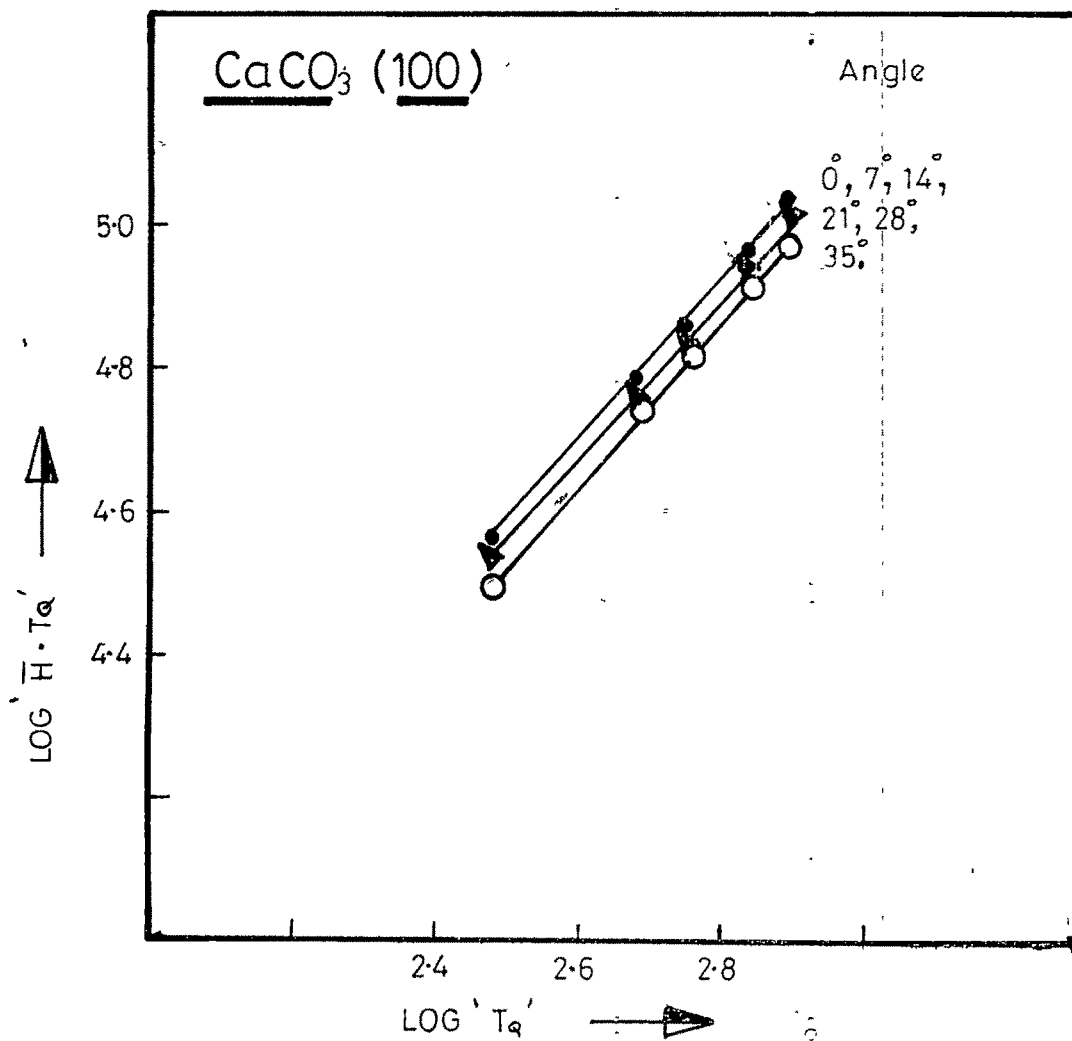


FIG. 5,4



Plot of Log 'H·Tα' vs Log 'Tα'

Fig: 5.5



## REFERENCES

1. Mott, B.L., 'Microindentation Hardness Testing', Butterworth Scientific Publications, London, Ch.1, (1956)
2. Saraf, C.L., Ph.D. Thesis, M.S. University of Baroda, Baroda, (1971)
3. Mehta, B.J., Ph.D. Thesis, M.S. University of Baroda, Baroda, (1972)
4. Shah, R.T., Ph.D. Thesis; M.S. University of Baroda, Baroda, (1976)
5. Acharya, C.T., Ph.D. Thesis, M.S. University of Baroda, Baroda, (1978)
6. Bhagia, L.J., Ph.D. Thesis, M.S. University of Baroda, Baroda, (1982)
7. Shah, A.J., Ph.D. Thesis, M.S. University of Baroda, Baroda, (1984)
8. Patel, M.B., Ph.D. Thesis, M.S. University of Baroda, Baroda, (1987)
9. Shah, A.J., Bhagia, L.J. and Pandya, J.R., Journal of the M.S. University of Baroda, Vol 31-32, No.3, P.85, (1982).